Accepted Manuscript

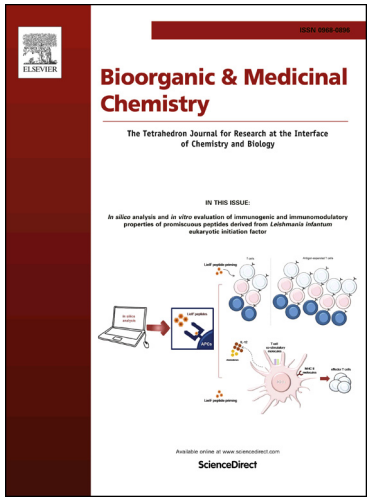

Discovery of orally efficacious RORγt inverse agonists. Part 2: Design, synthesis, and biological evaluation of novel tetrahydroisoquinoline derivatives

Mitsunori Kono, Tsuneo Oda, Michiko Tawada, Takashi Imada, Yoshihiro Banno, Naohiro Taya, Tetsuji Kawamoto, Hidekazu Tokuhara, Yoshihide Tomata, Naoki Ishii, Atsuko Ochida, Yoshiyuki Fukase, Tomoya Yukawa, Shoji Fukumoto, Hiroyuki Watanabe, Keiko Uga, Akira Shibata, Hideyuki Nakagawa, Mikio Shirasaki, Yasushi Fujitani, Masashi Yamasaki, Junya Shirai, Satoshi Yamamoto

PII: S0968-0896(17)31988-0
DOI: https://doi.org/10.1016/j.bmc.2017.12.008
Reference: BMC 14113

To appear in: *Bioorganic & Medicinal Chemistry*

Received Date: 11 October 2017
Revised Date: 30 November 2017
Accepted Date: 3 December 2017

Please cite this article as: Kono, M., Oda, T., Tawada, M., Imada, T., Banno, Y., Taya, N., Kawamoto, T., Tokuhara, H., Tomata, Y., Ishii, N., Ochida, A., Fukase, Y., Yukawa, T., Fukumoto, S., Watanabe, H., Uga, K., Shibata, A., Nakagawa, H., Shirasaki, M., Fujitani, Y., Yamasaki, M., Shirai, J., Yamamoto, S., Discovery of orally efficacious RORγt inverse agonists. Part 2: Design, synthesis, and biological evaluation of novel tetrahydroisoquinoline derivatives, *Bioorganic & Medicinal Chemistry* (2017), doi: https://doi.org/10.1016/j.bmc.2017.12.008

Discovery of orally efficacious RORγt inverse agonists. Part 2: Design, synthesis, and biological evaluation of novel tetrahydroisoquinoline derivatives

Mitsunori Kono,[a] *Tsuneo Oda,*[a] *Michiko Tawada,*[a] *Takashi Imada,*[a] *Yoshihiro Banno,*[a,b] *Naohiro Taya,*[a,b] *Tetsuji Kawamoto,*[a,b] *Hidekazu Tokuhara,*[a,b] *Yoshihide Tomata,*[a] *Naoki Ishii,*[a] *Atsuko Ochida,*[a] *Yoshiyuki Fukase,*[a,c] *Tomoya Yukawa,*[a] *Shoji Fukumoto,*[a,d] *Hiroyuki Watanabe,*[a] *Keiko Uga,*[a] *Akira Shibata,*[a] *Hideyuki Nakagawa,*[a] *Mikio Shirasaki,*[a,b] *Yasushi Fujitani,*[a] *Masashi Yamasaki,*[a,b] *Junya Shirai,*[a,e] *and Satoshi Yamamoto*[a]

[a] *Pharmaceutical Research Division, Takeda Pharmaceutical Company Limited, 26-1 Muraoka-Higashi 2-chome, Fujisawa, Kanagawa 251-8555, Japan*

ABSTRACT

A series of tetrahydroisoquinoline derivatives were designed, synthesized, and evaluated for their potential as novel orally efficacious retinoic acid receptor-related orphan receptor-gamma t (RORγt) inverse agonists for the treatment of Th17-driven autoimmune diseases. We carried out cyclization of the phenylglycinamide core by structure-based drug design and successfully identified a tetrahydroisoquinoline carboxylic acid derivative **14** with good biochemical binding and cellular reporter activity. Interestingly, the combination of a carboxylic acid tether and a central fused bicyclic ring was crucial for optimizing PK properties, and the compound **14**

showed significantly improved PK profile. Successive optimization of the carboxylate tether led to the discovery of compound **15** with increased inverse agonistic activity and an excellent PK profile. Oral treatment of mice with compound **15** robustly and dose-dependently inhibited IL-17A production in an IL23-induced gene expression assay.

KEYWORDS: Retinoic acid receptor-related orphan receptor-gamma t (RORγt), inverse agonist, autoimmune disease, Th17, IL-17, tetrahydroisoquinoline

ABBREVIATIONS: ROR t, retinoic acid receptor-related orphan receptor-gamma t; EAE, experimental autoimmune encephalomyelitis; BODIPY, boron-dipyrromethene; TR-FRET, time-resolved fluorescence resonance energy transfer; SAR, structure-activity relationship; IFN- , interferon- ; PBS, phosphate buffered saline; SBDD, structure-based drug design; PK, pharmacokinetics; PD, pharmacodynamics; AUC, area under the plasma concentration-time curve; *F*, bioavailability

*Corresponding author. Tel: +81-466-32-1108. Fax: +81-466-29-4455;

e-mail: mitsunori.kouno@takeda.com

Current affiliation.

[b] *Axcelead Drug Discovery Partners, Inc., 26-1, Muraoka-Higashi 2-Chome, Fujisawa, Kanagawa 251-0012, Japan*

[c] *Tri-Institutional Therapeutics Discovery Institute, Inc., 413 East 69th Street, New York, NY 10021, U.S.A.*

[d] *Japan Tobacco Inc., Central Pharmaceutical Research Institute, 1-1 Murasaki-cho, Takatsuki, Osaka, 569-1125, Japan.*

[e] *Cardurion Pharmaceuticals K.K. c/o Shonan Research Center, Takeda Pharmaceutical Company Ltd. 26-1, Muraoka-Higashi 2-chome Fujisawa, Kanagawa 251-8555, Japan*

Introduction

The Th17 cells, and the inflammatory cytokines they produce (IL-17A, IL-17F, etc.) play a central role in the pathogenesis of various autoimmune diseases such as inflammatory bowel disease, rheumatoid arthritis, multiple sclerosis, and psoriasis.[1–5] The biologics targeting IL-17A and IL-17A receptor have demonstrated clinical efficacy in psoriasis, rheumatoid arthritis, and uveitis.[6–8] Therefore, targeting Th17 cells has emerged as an attractive therapeutic intervention for these immune-related diseases.

Retinoic acid receptor-related orphan receptor-gamma t (RORγt), which is one of the orphan nuclear receptors, is a master regulator of Th17, IL-17, and IL-17/IFN-γ co-producing cells (Th1/17 cells) differentiation.[9,10] Expression of the RORγt is thought to be restricted to lymphoid organs, such as the thymus.[11] RORγt contributes to the expression of not only IL-17A, but also other pro-inflammatory factors such as IL-17F, IL-22, IL-23 receptor, and granulocyte macrophage colony-stimulating factor, secreted from various immune cells (e.g., Th17, Th1/17, innate lymphoid cells, and γδ T cells).[12,13] Deletion of RORγt results in impaired differentiation of murine and human Th17 cells. RORγt knockout mice are resistant to various autoimmune disease models such as colitis and experimental autoimmune encephalomyelitis (EAE). Therefore, inhibition of RORγt is expected to show treatment effects on various autoimmune diseases by suppressing differentiation and activation of Th17 and Th1/17 cells.

Recently, a large number of RORγt inhibitors have been reported from many research groups (**Figure 1**). It was first reported that natural products such as digoxin (**1**) and ursolic acid (**2**) inhibited RORγt and Th17 cell differentiation as an antagonist, and ameliorated EAE symptoms in mice by the intraperitoneal administration.[14,15] After that, many synthetic small molecular RORγt inverse agonists have been disclosed in the literatures and patents.[16–19] Among them, some compounds such as VTP-43742, JNJ-3534, ARN-6039, ADZ-0284, and JTE-451 are under clinical trials.[20–23] Examples of the structures of known RORγt inverse agonists (**3**-**7**) are shown in **Figure 1**.

Previously, we reported a series of phenylglycinamide derivatives as a novel class of ROR t inverse agonists having a unique binding mode.[24] Compound **8a** (**Figure 1**) showed potent in vitro ROR t inverse agonistic activity and moderate pharmacokinetic (PK) profile, and demonstrated inhibitory effect in a mouse IL23-induced IL-17A expression assay at a dose of 100 mg/kg, p.o. For further enhancement of in vivo potency, we embarked the exploration of the second generation chemotypes with superior in vitro activity and PK profile.

Herein, we report the design and synthesis of novel tetrahydroisoquinoline derivatives as potent and orally available ROR t inverse agonists obtained from the cyclization of the central phenylglycinamide core of compound **8a** by structure-based design, and subsequent optimization of right-hand acyl moiety. Furthermore, the biological activities and in vivo pharmacodynamic (PD) efficacy of compound **15** in mice are described.

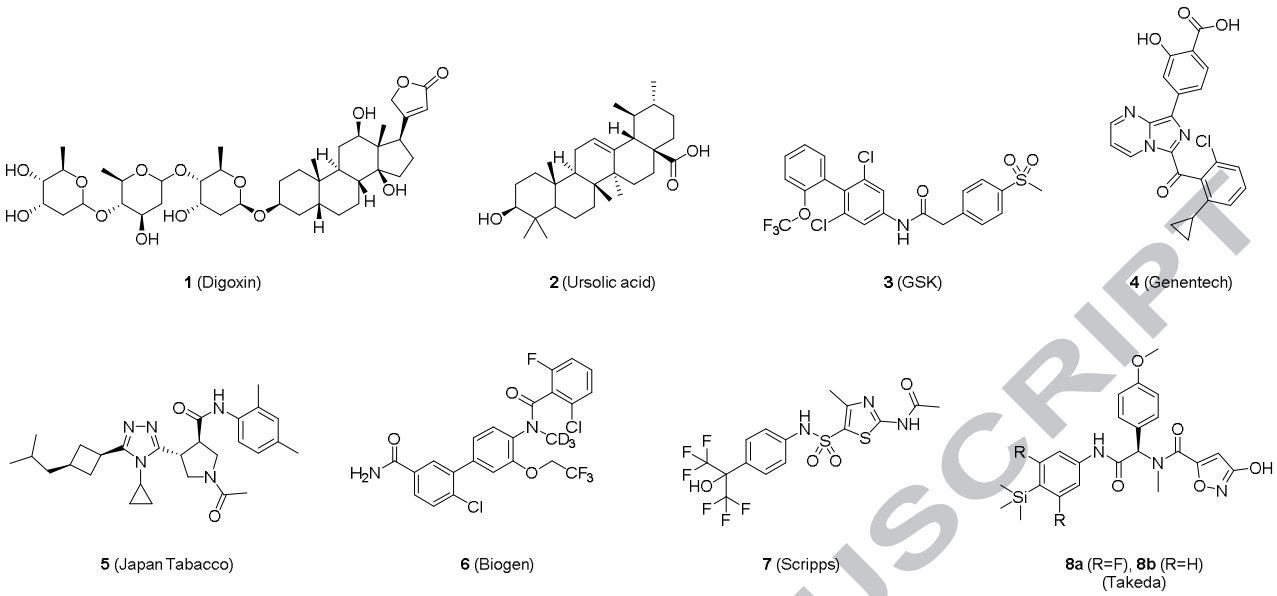

Figure 1. Chemical structures of reported ROR t inhibitors

Result and Discussion

Design Strategy Starting with Phenylglycine Derivative. For further enhancement of in vivo potency of the phenylglycinamide series, we initially focused on the flexible central diamide structure and hypothesized that reducing rotatable bond to rigidify the molecule would improve in vitro potency and PK profile.[25] In the course of optimizing phenylglycinamide derivatives, we succeeded in determining the crystal structure of ROR t protein in complex with phenylglycinamide analogue **8b**. According to the crystal structure[24], it was indicated that the central phenyl ring could be connected with the *N*-methyl amide moiety by some linkers without affecting the tridental conformation of the entire molecule including the key interactions with near amino acid residues (**Figure 2**). Hence, we focused on cyclization between the central phenyl ring and *N*-methyl amide moiety, and designed tetrahydroisoquinoline (**Y**) and the 1,4-benzoxazepine (**Z**) scaffold as novel bicyclic compounds which enable to reduce free rotatable bonds and thereby rigidify the structure (**Figure 3**).

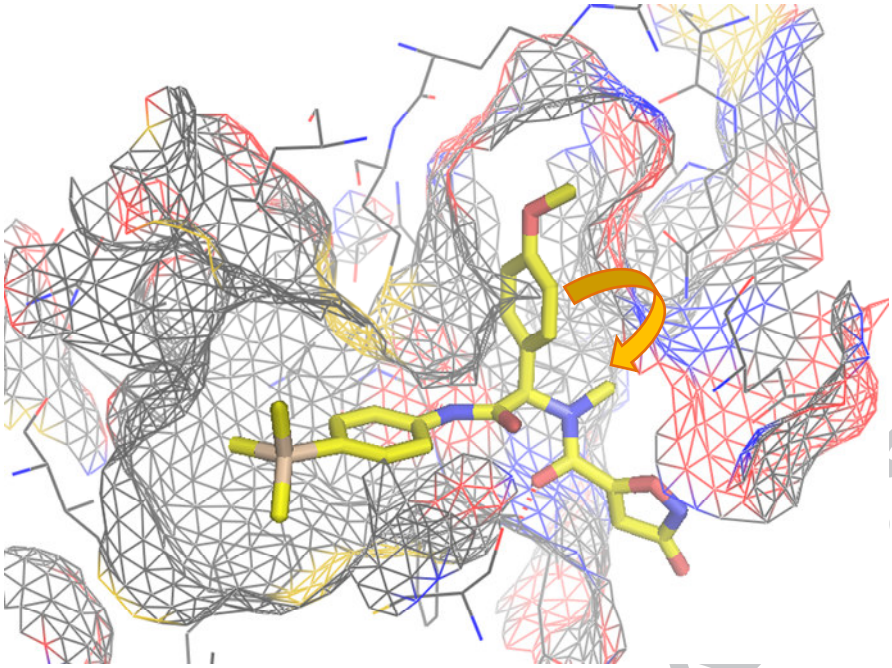

Figure 2. Surface view of the crystal structure of ROR t protein in complex with phenylglycinamide analogue **8b**.

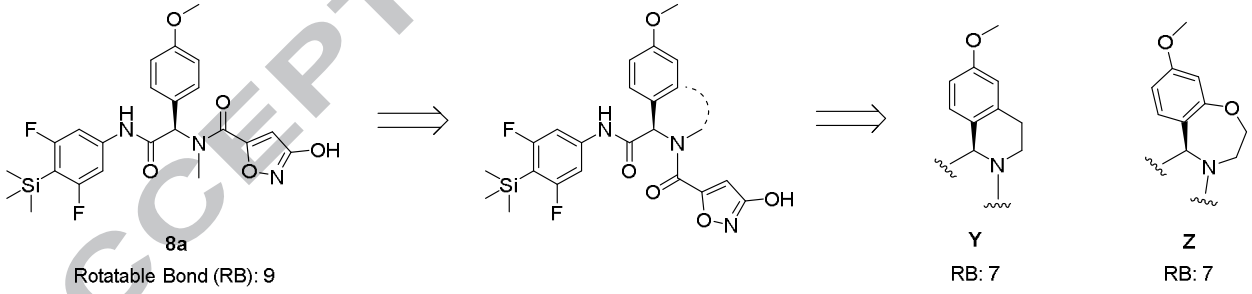

Figure 3. Cyclization strategy starting from the phenylglycinamide core and designed scaffolds

Initial SAR and Design Concept Validation. The synthesized compounds were initially evaluated using a RORγt biochemical binding assay and a RORγt jurkat cellular reporter gene assay. In the binding assay (cell-free system), our original ligand with BODIPY label was used

for evaluating the affinity of the test compounds for human RORγt by time-resolved fluorescence resonance energy transfer (TR-FRET) technology. In the reporter gene assay (cell-based), human Jurkat cells were used for evaluating the functional ability of the test compounds to affect transcriptional activity of RORγt by measuring luciferase activity. The PK profiles of the compounds were evaluated in mouse cassette-dosing tests. The in vivo PD efficacy of selected compounds was assessed by the action on IL-23-induced gene expression in mice.

First, we examined the cyclization of phenylglycinamide derivative **8a** into six-membered tetrahydroisoquinoline derivative **9** and seven-membered 1,4-benzoxazepine derivative **10**. The results are summarized in **Table 1**. As we expected, cyclization to the bicyclic core from phenylglycinamide did not affect the biochemical and cellular potencies, and the compound **9** showed slightly improved cellular reporter activity and equipotent binding activity to compound **8a**. In addition to the [6,6]-fused ring, the [6,7]-fused 1,4-benzoxazepine derivative **10** also showed tolerable biochemical binding and cellular reporter activity. However, conversion to compound **10** resulted in a much poorer PK profile compared with phenylglycinamide **8a**.

Along with the central core modification, we also conducted the transformation of the hydroxyisoxazole moiety. In our previous efforts, we found that the hydroxyisoxazole group was suitable for the acyl moiety in the phenylglycinamide series. The 3-hydroxyisoxazole group is a commonly known carboxylic acid bioisostere, and widely used in medicinal chemistry drug design.[26] Thus, we conducted introduction of a carboxylic acid group by bioisosteric transformation of the acyl moiety. Although the carboxylic acid derivative **12** had slightly decreased reporter activity in spite of potent binding, the compound showed remarkable improvement of plasma exposure and oral availability. It was of interest that there is no significant difference in the PK profile between hydroxyisoxazole and carboxylic acid derivatives of phenylglycinamide compounds (**8a** vs **11**). It was also found that the ring closure

of the phenylglycinamide **8a** to form the tetrahydroisoquinoline did not increase plasma exposure (**9**). These results suggested that the combination of the carboxylic acid moiety and central fused bicyclic ring is very important for the PK profile. Thus, we successfully conducted scaffold exchange of phenylglycinamide derivatives and generated a new [6,6]-fused ring core scaffold of ROR t inverse agonist. We decided to focus on the tetrahydroisoquinoline carboxylic acid derivatives and conducted further optimization on the acyl tether.

Table 1. In vitro activities and their PK profiles of derivatives modifying core scaffold and acyl tether

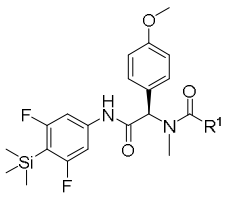

X

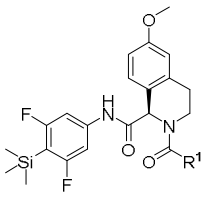

Y

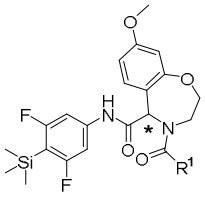

Z

compound	Scaffold	R^1	Binding[a] IC_{50} (nM) [95%CI][c]	Reporter gene[b] IC_{50} (nM) [95%CI][c]	mouse PK[d] AUC_{0-8h} (ng·h/mL)	mouse PK[d] F (%)
8a	X	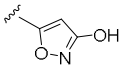	4.3 [3.4-5.5]	13 [10-16]	374	18
9	Y	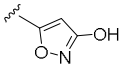	5.3 [4.7-5.9]	6.1 [3.6-11]	200	11
10[e]	Z	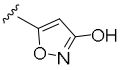	2.8 [2.5-3.1]	40 [20-83]	29.5	9.0
11	X	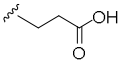	7.5 [5.9-9.5]	220 [150-310]	162	8.5
12	Y	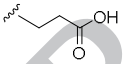	4.2 [3.6-4.8]	54 [42-70]	2500	51

[a] Displacement assay of BODIPY-labeled ligand with apo RORγt [b] Inhibition of RORγt transcriptional activity human Jurkat cells
[c] 95% confidence intervals (CI) conducted in duplicate (n = 2) [d] The values shown as means of three determinations (1 mg/kg, po)
[e] Compound **10** is eutomer

Optimization of carboxylic acid tether moiety. The SAR trends from the study on the acyl tether are described in **Table 2**. Initially, we attempted to fix the conformation of the tether and designed α,β-unsaturated carboxylic acids (**13** and **14**). The *trans*-isomer **14** possessed comparable binding and reporter activity to compound **12**, whereas the *cis*-isomer **13** resulted in slight loss of binding and reporter activity. However, plasma exposure of compound **14** was not as large as that of compound **12**. Next, we investigated the linker length (compound **12** possesses two atoms between carbonyl and carboxylate). The three-atom-linker analog **15** and the four-atom-linker analog **16** showed equipotent activity to **12**. Interestingly, one carbon elongation had

a dramatic impact on PK profile, and the compound **15** demonstrated high plasma exposure and excellent bioavailability. Replacement of the carboxylic acid with a carbamoyl group (**17**) led to an increase of biochemical potency, and **17** showed the most potent reporter activity in this series. However, the non-acidic substituent resulted in a poor PK profile. On the basis of these results, we focused on the three atom linker and performed linker modification. Regarding the introduction of a methyl group, the monomethyl analog **18** retained potent binding and reporter activity and good PK profile whereas the *gem*-dimethyl analog **19** showed decreased reporter activity. Replacement of the methyl group of **19** with a hydroxy group restored reporter activity, but the plasma exposure was decreased (**20**). In addition to substituent introduction, we changed the linker from carbon to oxygen or nitrogen. However, these modifications resulted in decrease of reporter activity (**21** and **22**). As for further bioisosteric transformation, thiazolidinedione instead of carboxylic acid showed potent activities, but the PK profile got worse (**23**). From these results, we concluded that compound **15** was the best compound in the tetrahydroisoquinoline series, and we selected **15** for further in vivo biological evaluation.

Table 2. In vitro activities and their PK profiles of derivatives modifying the acyl tether

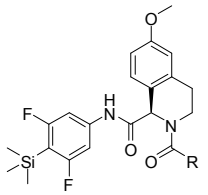

compound	R	Binding[a]	Reporter gene[b]	mouse PK[d]	
		IC_{50} (nM) [95%CI][c]	IC_{50} (nM) [95%CI][c]	$AUC_{0\text{-}8h}$ (ng·h/mL)	*F* (%)
12	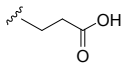	4.2 [3.6-4.8]	54 [41-70]	2500	51
13	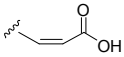	17 [10-27]	320 [260-410]	N.T.	N.T.
14	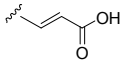	4.1 [3.4-4.9]	38 [29-49]	619	51
15	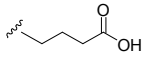	3.0 [2.4-3.8]	23 [19-29]	6894	94
16	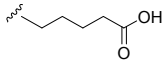	6.6 [5.6-7.8]	24 [19-31]	1031	84
17	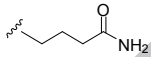	3.1 [2.3-4.0]	6.7 [4.7-9.6]	92	14
18	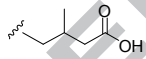	3.8 [3.1-4.7]	19 [12-30]	2498	65
19	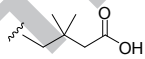	5.6 [4.9-6.5]	46 [28-78]	2273	40
20	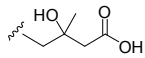	4.5 [3.8-5.3]	32 [25-41]	159	34
21	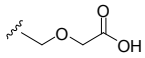	3.5 [3.0-4.0]	140 [97-190]	N.T.	N.T.
22	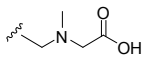	7.8 [6.5-9.4]	220 [150-320]	N.T.	N.T.
23	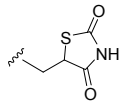	7.6 [6.4-9.2]	41 [28-62]	120	13

[a] Displacement assay of BODIPY-labeled ligand with apo RORγt [b] Inhibition of RORγt transcriptional activity human Jurkat cells [c] 95% confidence intervals (CI) conducted in duplicate (n = 2) [d] The values shown as means of three determinations (1 mg/kg, po)

In vivo PD Study and PK Profile of Compound 15. To determine whether a ROR t inverse agonist could modulate the cytokine production through suppressing differentiation and activation of Th17 and Th1/17 cells, an in vivo mouse PD model was developed. We established Mea mouse IL-23-induced cytokine expression model.[27] This PD model was used to evaluate the effect of the compounds on IL-23-induced IL-17A expression in the ears of mice. The results are shown in **Figure 5**. Compound **15** showed robust and dose-dependent inhibition of IL-17A expression after oral administration at 3, 10, and 30 mg/kg (ED_{50}= 2.8 mg/kg). On the other hand, we also investigated the expression of IFN- which is not regulated by ROR t as for counter assay, and compound **15** did not affect the expression of IFN- (data not shown). Moreover, the tetrahydroisoquinoline series represented a significant improvement of in vivo PD efficacy relative to phenylglycinamide derivative **8a**, which showed PD efficacy only at a dose of 100 mg/kg, p.o.. In parallel with the PD assay, we measured the plasma concentration of compound **15** after oral administration. Compound **15** demonstrated excellent PK profile in mice, high maximum plasma concentration (Cmax: 1.63, 7.72, 19.0 μg/mL), and plasma exposure ($AUC_{0\text{-}24h}$: 10.7, 48.0, 159 μg·h/mL) increased in a dose-dependent manner (at dose of 3, 10, 30 mg/kg, p.o.).

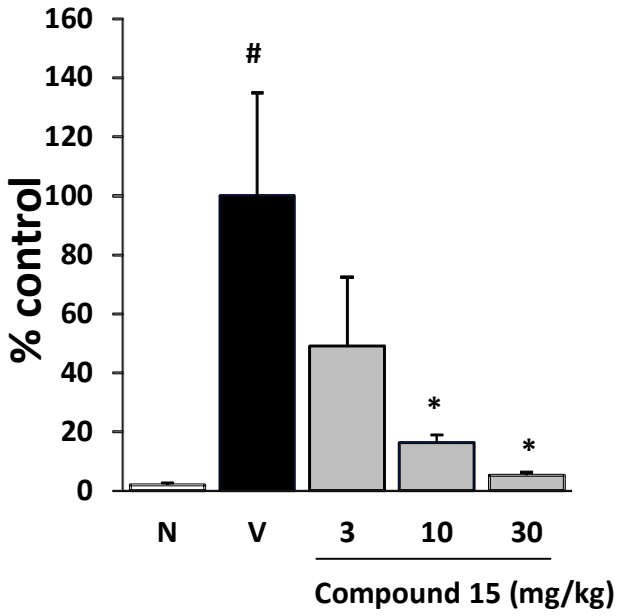

Figure 5. Assessment of **15** in mice IL-23-induced cytokine expression PD assay. Data are represented as the mean values ± s.e. of 7 separate experiments. N indicates the PBS-injected and V indicates the IL-23-injected and vehicle-administered control group. #$p \leq 0.05$ (Aspin-Welch test) compared with PBS-treated group (N) *$p \leq 0.025$ (one-tailed Shirley Williams' test) compared to the IL-23-injected and vehicle-administered group (V).

Chemistry.

Synthesis of the tetrahydroisoquinoline-aniline unit[28] is described in **Scheme 1**. 3-Methoxyphenethylamine **24** was reacted with glyoxylic acid ethyl ester in the presence of HBr to afford tetrahydroisoquinoline ethyl ester **25**. Boc protection and *O*-methylation proceeded smoothly, and subsequent hydrolysis by using LiOH gave the carboxylic acid **28**. Amidation with a poor nucleophilic 3,5-difluoro-4-trimethylsilylaniline was achieved by using propylphosphonic acid anhydride cyclic trimer (T3P) in the presence of a stoichiometric amount of DMAP to obtain racemic intermediate **29**.

Scheme 1[a]

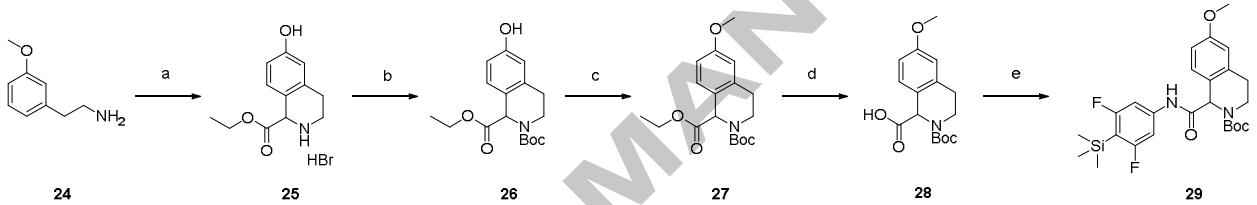

[a]Reagents and conditions: (a) glyoxilic acid ethyl ester, HBr, EtOH, reflux, 70%; (b) Boc_2O, Et_3N, THF, H_2O, rt, 87%; (c) MeI, Cs_2CO_3, DMF, rt, 96%; (d) LiOH, THF, EtOH, rt, 94%; (e) 3,5-difluoro-4-trimethylsilyl aniline, T3P, DMAP, EtOAc, 80 °C, 60%

Synthesis of target compounds **15** and **34,** and the determination of absolute configuration for the tetrahydroisoquinoline-aniline unit were illustrated in **Scheme 2**. First, we conducted chiral HPLC resolution of the racemate **29** and prepared the optically pure compounds **30** and **32**. Deprotection of amino group was carefully conducted in short time due to the instability of trimethylsilyl group under acidic conditions, and the chiral amines **31** and **33** were obtained. The target compounds (**15** and **34**) were synthesized from compounds **31** and **33** by the reaction with glutaric acid anhydride. The absolute configuration of **31** was determined as (*R*)-configuration by X-ray crystallographic analysis of compound **31** tartrate (**Figure 5**). Therefore, the eutomer **15** was proved to be (*R*)-configuration.

Scheme 2[a]

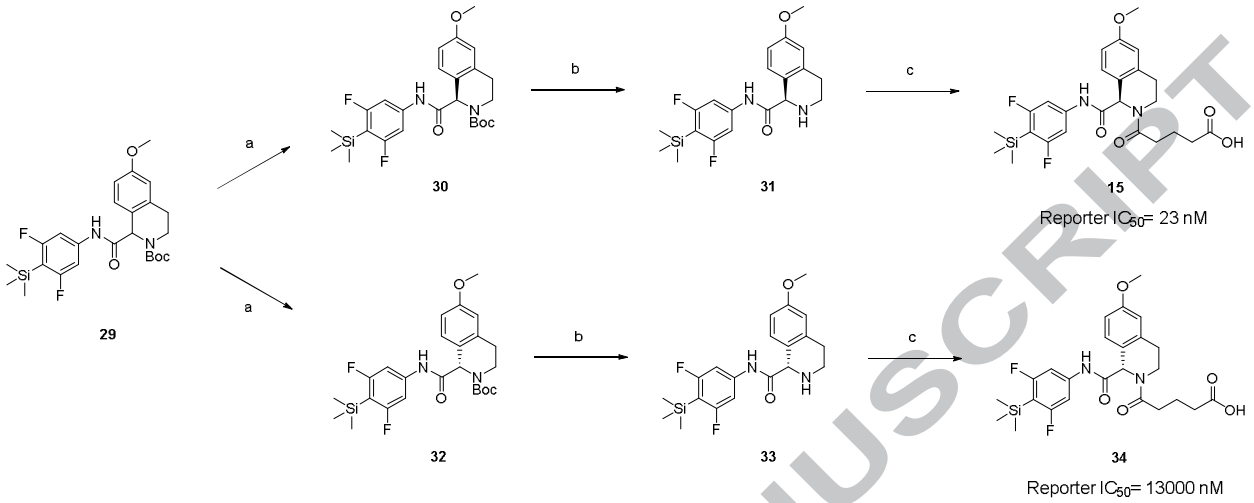

[a]Reagents and conditions: (a) prep. HPLC, CHIRALPAK AD, hexane/EtOH, 42% for **30** and 44% for **32**; (b) TFA, rt, 93% for **31** and 91% for **33**; (c) glutaric anhydride, Et_3N, THF, 56% for **15** and 49% for **34**

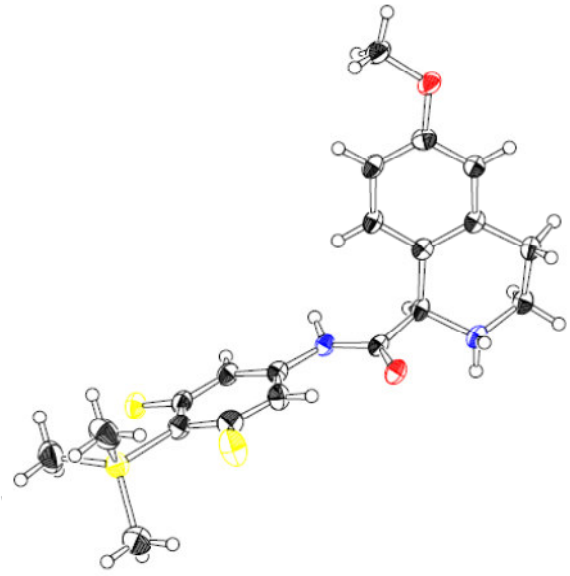

Figure 6. ORTEP of tartrate of compound **31**, thermal ellipsoids are drawn at 50% probability.

Synthesis of the target compounds is described in **Scheme 3**. The final compounds **9**, **11-16**, and **18**-**23** were afforded via acylation with the corresponding carboxylic acids or reaction with the corresponding acid anhydrides. Carboxamide derivative **17** was obtained by amidation from **15** using HATU and ammonium chloride.

Scheme 3[a]

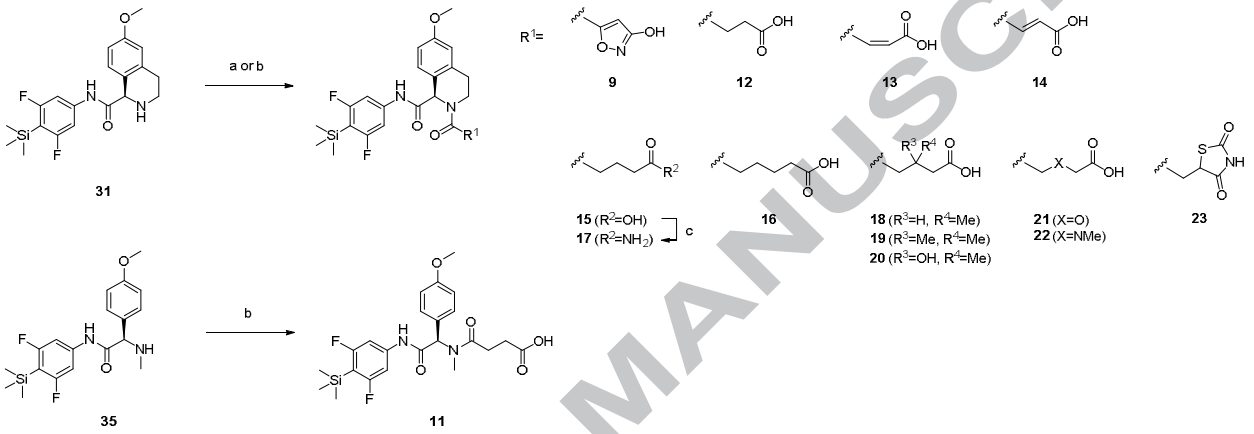

[a]Reagents and conditions: (a) R^1-CO_2H, HATU, $^iPr_2NEt$, DMF, 12–52% for **9**, **13**, **14**, **23**; (b) acid anhydrides, Et_3N, THF, 29–95% for **12**, **15**, **16**, **18**-**22**; (c) ammonium chloride, HATU, $^iPr_2NEt$, DMF, 57%

Preparation of the benzoxazepine derivative **10** is illustrated in **Scheme 4**. Boc protection of *N*-benzylethanolamine **36** gave the compound **37**. The Mitsunobu reaction with 3-methoxyphenol using DIAD and PPh_3, and subsequent deprotection provided the intermediate **39**. In situ generation of methylbromo(methoxy)acetate followed by the reaction with **39** afforded a coupling product **40**. The benzoxazepine scaffold was then constructed by TMSCl-promoted intramolecular cyclization[29] at room temperature to yield compound **41**. The benzyl group was removed by hydrogenation using $Pd(OH)_2$-C, followed by protection with a Boc group and hydrolysis to give **43**. Amidation under the same conditions as synthesis of tetrahydroisoquinoline derivative afforded amide **44**. The racemate of **10** was synthesized by

acidic deprotection of **44** and subsequent acylation with 3-hydroxyisoxazole-5-carboxylic acid. The target eutomer was obtained by chiral HPLC resolution and gave the optically pure compound **10**.

Scheme 4[a]

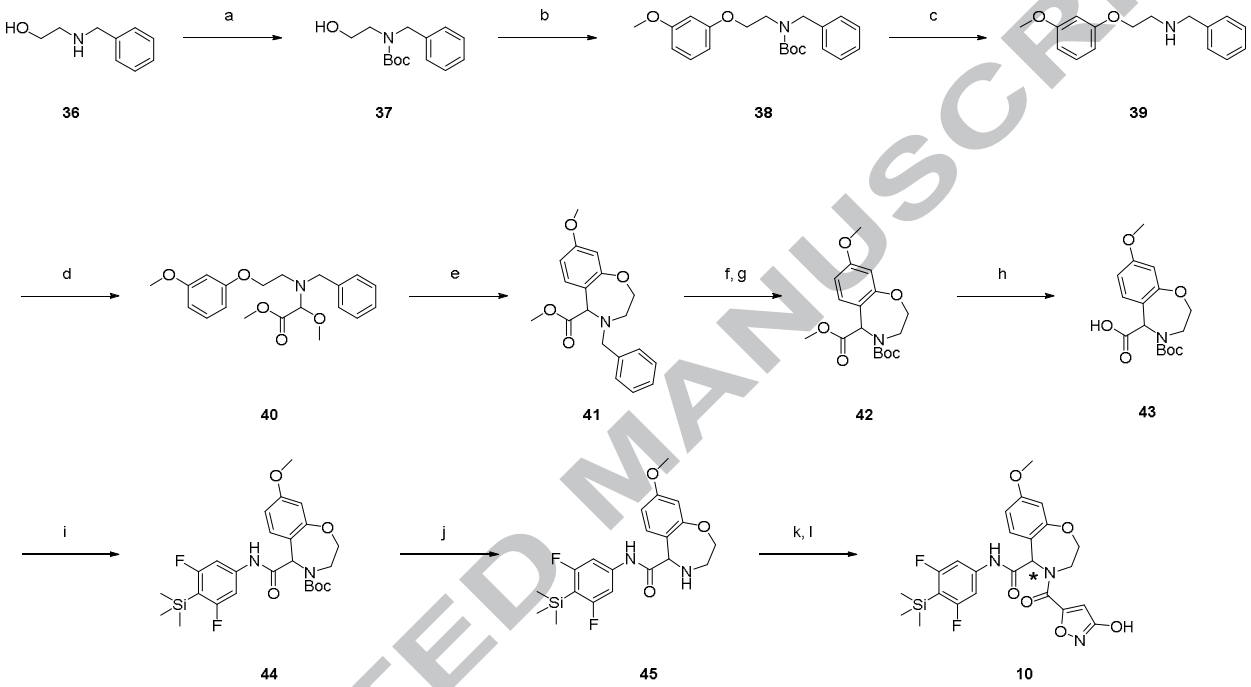

[a]Reagents and conditions: (a) $(Boc)_2O$, THF, rt, quant.; (b) 3-methoxyphenol, DIAD, PPh_3, THF, 0 °C–rt, 41%; (c) TFA, 0 °C–rt, quant.; (d) methyl methoxyacetate, NBS, AIBN/$PhCF_3$, $^iPr_2NEt$, THF, rt, 76%; (e) TMSCl, MeCN, 0 °C–rt, 60%; (f) H_2, $Pd(OH)_2$-C, MeOH, rt, 96%; (g) $(Boc)_2O$, THF, rt, quant. 77% from **42**; (h) LiOH, MeOH-THF, rt, 94%; (i) 3,5-difluoro-4-trimethylsilyl aniline, T3P, DMAP, EtOAc, 80 °C, 81%; (j) TFA, rt, 88%; (k) 3-hydroxyisoxazole-5-carboxylic acid, HATU, $^iPr_2NEt$, DMF, 41%; (l) prep. SFC, CHIRALPAK AS-H, CO_2/EtOH, 30%

Conclusion

In the course of our exploration of novel RORγt inverse agonists that are therapeutically effective against various autoimmune diseases, we designed, synthesized, and evaluated a series of tetrahydroisoquinoline derivatives. Cyclization of the phenylglycinamide core by SBDD

approach successfully delivered a novel bicyclic scaffold with tolerable biochemical binding and cellular reporter activity. Combination of a carboxylic acid tether and a tetrahydroisoquinoline scaffold resulted in significant improvement of the PK profile. The optimization of the acyl tether led to the discovery of 5-((1*R*)-1-((3,5-difluoro-4-(trimethylsilyl)phenyl)carbamoyl)-6-methoxy-3,4-dihydroisoquinolin-2(1*H*)-yl)-5-oxopentanoic acid (**15**), a potent, and orally active RORγt inverse agonist with excellent PK profile. Oral administration of compound **15** to mice robustly and dose-dependently inhibited IL-17A production in an IL23-induced gene expression assay. The results suggested that our potent and selective RORγt inverse agonists would become a beneficial agent for the treatment of Th17-driven autoimmune diseases.

Experimental section

Chemistry

Reagents and solvents were obtained from commercial sources and used without further purification. Reaction progress was determined by thin layer chromatography (TLC) analysis on Merck Kieselgel 60 F254 plates or Fuji Silysia NH plates. Silica gel column chromatography was performed on Purif-Pack (SI or NH, SHOKO SCIENTIFIC). Proton nuclear magnetic resonance (1H NMR) spectra were recorded on Bruker Ultra Shield-300 (300 MHz) instruments. Chemical shifts are given in parts per million (ppm) with tetramethylsilane as an internal standard. Abbreviations are used as follows: s = singlet, d = doublet, t = triplet, q = quartet, m = multiplet, dd = doublets of doublet, br = broad. Coupling constants (J values) are given in hertz (Hz). LC–MS analysis was performed on a Shimadzu LC-20AD separations module or Agilent 1200 series, operating in ESI (+ or -) ionization mode. Analytes were eluted using a linear gradient of 0.05% TFA containing H_2O/CH_3CN or 0.01% TFA containing H_2O/CH_3CN or 5 mM ammonium acetate containing H_2O/CH_3CN or 10 mM NH_4HCO_3 containing H_2O/CH_3CN or 0.01% heptafluorobutyric acid /1.0% isopropyl alcohol containing H_2O/CH_3CN mobile phase. Preparative HPLC was performed on a Waters 2525 separations module (L-column2 ODS (20 x150 mm I.D., CERI, Japan); MS spectra were recorded using a Waters ZQ2000 with electrospray ionization or on a GILSON system, equipped with a L-column2 ODS (20 x150 mm I.D., CERI, Japan) or on Waters Deltaprep 300 system or on Shimadzu 10A VP system. Samples were eluted using a linear gradient of 0.1% TFA in H_2O/CH_3CN or 10 mM NH_4HCO_3 in H_2O /CH_3CN, or H_2O/CH_3CN. Purity data were collected by a HPLC with Corona CAD (Charged Aerosol Detector), Nano quantity analyte detector (NQAD), or photo diode array detector. The column was a Capcell Pak C18AQ (50 mm x 3.0 mm I.D., Shiseido, Japan) or L-column 2 ODS (30 mm x 2.0 mm I.D., CERI, Japan) with a temperature of 50 °C and a flow rate of 0.5 mL/min.

Mobile phase A and B under a neutral condition were a mixture of 50 mM Ammonium acetate, H_2O and CH_3CN (1:8:1, v/v/v) and a mixture of 50 mM ammonium acetate and CH_3CN (1:9, v/v), respectively. The ratio of mobile phase B was increased linearly from 5% to 95% over 3 min, 95% over the next 1 min. Mobile phase A and B under an acidic condition were a mixture of 0.2% formic acid in 10 mM ammonium formate and 0.2% formic acid in CH_3CN, respectively. The ratio of mobile phase B was increased linearly from 14% to 86% over 3 min, 86% over the next 1 min.

Ethyl 6-hydroxy-1,2,3,4-tetrahydroisoquinoline-1-carboxylate hydrobromide (25). 48 % Hydrobromic acid (101 g, 600 mmol) was added dropwise (over a period of 10 min) to *m*-methoxyphenethylamine (22.68 g, 150 mmol) at room temperature. After being stirred at 120 °C for 12 h, the reaction mixture was diluted with EtOH (200 ml) and concentrated in vacuo. The evaporation was repeated after the addition of toluene (200 ml, 4 times) to give white solid. The residue was dissolved in EtOH (150 ml), and 47 % glyoxylic acid ethyl ester (polymer form) (35.8 g, 165 mmol) was added thereto. After being refluxed for 15 h, the reaction mixture was concentrated in vacuo. The evaporation was repeated after the addition of toluene (200 ml, twice). The residual oil was diluted with EtOAc (200 ml) and sitrred at room temperature for 40 min to give crystals, which were collected by filtration and washed with EtOAc to give **25** (31.8 g, 70 %) as a pale yellow solid. ^{1}H NMR (300 MHz, DMSO-d_6) 1.26 (3H, t, J = 7.2 Hz), 2.86 – 2.99 (2H, m), 3.35 – 3.61 (4H, m), 4.19 – 4.35 (2H, m), 5.35 (1H, s), 6.63 (1H, d, J = 2.6 Hz), 6.73 (1H, dd, J = 8.7, 2.6 Hz), 7.23 (1H, d, J = 8.3 Hz), 9.40 (1H, brs), 9.69 (2H, brs). LC/MS m/z 222.2 (M + H).

2-*tert*-Butyl 1-ethyl 6-hydoxy-3,4-dihydroisoquinoline-1,2(1*H*)-dicarboxylate (26). To a solution of **25** (31.7 g, 105 mmol) in THF (300 ml) and water (80 ml) was added Et_3N (14.6 ml,

105 mmol) and Boc_2O (25.6 ml, 110 mmol) at room temperature. The mixture was stirred at room temperaturefor 1 h. The mixture was poured into water and extracted with EtOAc. The organic layer was separated, washed with brine, dried over $MgSO_4$ and concentrated in vacuo. The residue was purified by column chromatography (silica gel, eluted with 0%–50% EtOAc in hexane) to give **26** (29.5 g, 87 %) as a colorless oil. ^{1}H NMR (300 MHz, $CDCl_3$) 1.17 – 1.32 (4H, m), 1.45 – 1.53 (10H, m), 2.69 – 2.99 (2H, m), 3.62 – 3.83 (2H, m), 4.07 – 4.20 (2H, m), 4.93 – 5.03 (1H, m), 5.33 (1H, s), 6.63 (1H, s), 6.69 (1H, d, *J* = 8.7 Hz), 7.31 – 7.39 (1H, m). LC/MS m/z 222.1 (M + H – (Boc)).

2-*tert*-Butyl 1-ethyl 6-methoxy-3,4-dihydroisoquinoline-1,2(1*H*)-dicarboxylate (27). To a solution of **26** (6.43 g, 20 mmol) in DMF (50 ml) was added Cs_2CO_3 (7.82 g, 24.0 mmol) and MeI (2.50 ml, 40.0 mmol) at room temperature. The mixture was stirred at room temperature overnight. The mixture was poured into water and extracted with EtOAc. The organic layer was separated, washed with water and brine, dried over $MgSO_4$ and concentrated in vacuo. The residue was purified by column chromatography (NH silica gel, eluted with 0%–20% EtOAc in hexane) to give **27** (6.45 g, 96 %) as a colorless oil. ^{1}H NMR (300 MHz, $CDCl_3$) 1.16 – 1.31 (3H, m), 1.40 – 1.52 (9H, m), 2.71 – 3.02 (2H, m), 3.64 – 3.84 (5H, m), 4.07 – 4.20 (2H, m), 5.34 (1H, s), 6.68 (1H, s), 6.77 (1H, dd, *J* = 8.3, 2.6 Hz), 7.35 – 7.45 (1H, m).

2-(*tert*-Butoxycarbonyl)-6-methoxy-1,2,3,4-tetrahydroisoquinoline-1-carboxylic acid (28). To a solution of **27** (6.37 g, 19 mmol) in THF (20 ml) and EtOH (20 ml) was added NaOH (19.0 ml, 38.0 mmol) at room temperature. The mixture was stirred at room temperature overnight. After evaporation of the solvent, the residue was neutralized with 2 *N* HCl at 0 °C and extracted with EtOAc. The organic layer was separated, washed with water and brine, dried over $MgSO_4$ and concentrated in vacuo to give **28** (5.50 g, 94 %) as a white amorphous solid. ^{1}H NMR (300

MHz, $CDCl_3$) 1.48 (3H, s), 1.44 (6H, s), 2.79 (1H, d, *J* = 15.9 Hz), 2.93 (1H, d, *J* = 15.9 Hz), 3.55 – 3.68 (1H, m), 3.68 – 3.91 (4H, m), 5.34 (1H, s), 6.68 (1H, d, *J* = 2.6 Hz), 6.77 (1H, dd, *J* = 8.5, 2.5 Hz), 7.38 (1H, d, *J* = 8.7 Hz). LC/MS m/z 208.1 (M + H – (Boc)).

***tert*-Butyl 1-((3,5-difluoro-4-(trimethylsilyl)phenyl)carbamoyl)-6-methoxy-3,4-dihydroisoquinoline-2(1*H*)-carboxylate (29).** To a mixture of 3,5-difluoro-4-(trimethylsilyl)aniline (1.05 g, 5.22 mmol), **28** (1.76 g, 5.74 mmol), DMAP (0.70 g, 5.74 mmol), and *N*,*N*'-diisopropylethylamine (4.56 ml, 26.1 mmol) in EtOAc (30 ml) was added T3P, 1.7 M solution in EtOAc (9.21 ml, 15.7 mmol). After being stirred at 80 °C for 2 h, the mixture was quenched with water at ambient temperature and extracted with EtOAc. The organic layer was separated, washed with 10 % aqueous citric acid, dried over $MgSO_4$ and concentrated in vacuo. The residue was triturated with Et_2O to give **29** (1.41 g, 55 %) as a white powder. ^{1}H NMR (300 MHz, $CDCl_3$) 1.52 (9H, s), 2.76 – 2.98 (2H, m), 3.51 – 3.75 (2H, m), 3.80 (3H, s), 5.58 (1H, brs), 6.73 (1H, d, *J* = 2.3 Hz), 6.81 (1H, dd, *J* = 8.3, 2.3 Hz), 6.97 – 7.07 (2H, m), 7.19 (1H, brs), 9.11 (1H, brs). LC/MS m/z 489.3 (M + H)

***tert*-butyl (1*R*)-1-((3,5-difluoro-4-(trimethylsilyl)phenyl)carbamoyl)-6-methoxy-3,4-dihydroisoquinoline-2(1*H*)-carboxylate (30).** Compound **29** (1.44 g) was subjected to preparative chiral HPLC (Column: CHIRALPAK AD, Eluent: Hexane/ethanol =850/150 (v/v), Flow rate: 60 mL/min, Pressure: 0.2 Mpa, Detector&sens.: UV220 nM, Temperature: 30 °C). The factions with a shorter retention time gave the title compound **30** (610 mg, 42%) with > 99%ee as colorless amorphous solid. LC/MS m/z 489.3 (M + H).

(1*R*)-*N*-(3,5-difluoro-4-(trimethylsilyl)phenyl)-6-methoxy-1,2,3,4-tetrahydroisoquinoline-1-carboxamide (31). Ice-cooled trifluoroacetic acid (5.0 ml, 1.24 mmol) was added to **30** (610 mg,

1.24 mmol) at room temperature. After being stirred at room temperature for 2 min, the reaction mixture was poured into iced saturated aqueous $NaHCO_3$ and extracted with EtOAc. The organic layer was dried over $MgSO_4$ and concentrated in vacuo to give **31** (450 mg, 93 %) as a colorless amorphous solid. This product was subjected to the next reaction without further purification. LC/MS m/z 389.2 (M – H)

5-((1*R*)-1-((3,5-difluoro-4-(trimethylsilyl)phenyl)carbamoyl)-6-methoxy-3,4-dihydroisoquinolin-2(1*H*)-yl)-5-oxopentanoic acid (15). A mixture of **31** (300 mg, 0.77 mmol), dihydro-2*H*-pyran-2,6(3*H*)-dione (131 mg, 1.15 mmol), TEA (0.214 ml, 1.54 mmol), and THF (6.0 ml) was stirrred at room temperature for 3 h. The mixture was concentrated in vacuo. The residue was purified by column chromatography (diol column, eluted with 50%–100% EtOAc in hexane) to give **15** (217 mg, 56 %) as a colorless amorphous solid. ^{1}H NMR (300 MHz, DMSO-d_6) 0.30 (9H, s), 1.64 – 1.85 (2H, m), 2.23 – 2.33 (2H, m), 2.36 – 2.62 (2H, m), 2.73 – 2.88 (1H, m), 3.05 –.19 (1H, m), 3.44 – 3.57 (1H, m), 3.73 (3H, s), 3.94 – 4.08 (1H, m), 5.58 – 5.64 (1H, m), 6.77 – 6.86 (2H, m), 7.15 – 7.25 (2H, m), 7.46 (1H, d, J = 9.1 Hz), 10.76 (1H, s), 12.03 (1H, s). LC/MS m/z 505.4 (M + H). Optical rotation: $[\alpha]^{25}_D$ –6.6 (c 0.250, MeOH). HPLC purity: 98.9%.

***tert*-butyl (1*S*)-1-((3,5-difluoro-4-(trimethylsilyl)phenyl)carbamoyl)-6-methoxy-3,4-dihydroisoquinoline-2(1*H*)-carboxylate (32).** Compound **29** (1.44 g) was subjected to preparative chiral HPLC (Column: CHIRALPAK AD, Eluent: Hexane/ethanol =850/150 (v/v), Flow rate: 60 mL/min, Pressure: 0.2 Mpa, Detector&sens.: UV220 nM, Temperature: 30 °C). The factions with a longer retention time gave the title compound **32** (630 mg, 44%) with > 99%ee as colorless amorphous solid. LC/MS m/z 489.3 (M + H).

(1*S*)-*N*-(3,5-difluoro-4-(trimethylsilyl)phenyl)-6-methoxy-1,2,3,4-tetrahydroisoquinoline-1-carboxamide (33). Compound **33** was prepared in a manner similar to that described for **31** in 91% yield as a colorless amorphous solid. LC/MS m/z 389.2 (M – H)

5-((1*S*)-1-((3,5-difluoro-4-(trimethylsilyl)phenyl)carbamoyl)-6-methoxy-3,4-dihydroisoquinolin-2(1*H*)-yl)-5-oxopentanoic acid (34). Compound **34** was prepared in a manner similar to that described for **15** in 49% yield as a colorless amorphous solid. ^{1}H NMR (300 MHz, DMSO-d_6) 0.29 (9H, s), 1.63 – 1.82 (2H, m), 2.18 – 2.32 (3H, m), 2.36 – 2.49 (1H, m), 2.52 – 2.61 (1H, m), 2.72 – 2.88 (1H, m), 3.05 – 3.19 (1H, m), 3.43 – 3.56 (1H, m), 3.73 (3H, s), 5.56 – 5.67 (1H, m), 6.77 – 6.86 (2H, m), 7.15 – 7.25 (2H, m), 7.46 (1H, d, J = 9.1 Hz), 10.76 (1H, s), 12.01 (1H, brs). LC/MS m/z 503.3 (M – H) Optical rotation: $[\alpha]^{25}_{D}$ +7.2 (c 0.252, MeOH). HPLC purity: 90.5%.

(1*R*)-*N*-(3,5-difluoro-4-(trimethylsilyl)phenyl)-2-((3-hydroxy-1,2-oxazol-5-yl)carbonyl)-6-methoxy-1,2,3,4-tetrahydroisoquinoline-1-carboxamide (9). To a stirred solution of **31** (158 mg, 0.40 mmol), *N*,*N*'-diisopropylethylamine (0.141 ml, 0.81 mmol), and 3-hydroxyisoxazole-5-carboxylic acid (54.8 mg, 0.42 mmol) in DMF (3.0 ml) was added HATU (185 mg, 0.49 mmol) at room temperature. The mixture was stirred at room temperature overnight, and the mixture was quenched with water and extracted with EtOAc. The organic layer was separated, washed with water and brine, dried over $MgSO_4$ and concentrated in vacuo. The residue was purified by column chromatography (silica gel, eluted with 20%–90%EtOAc in hexane) and crystallized from EtOAc–hexane to give **9** (53.5 mg, 26 %) as a colorless amorphous solid. ^{1}H NMR (300 MHz, DMSO-d_6) 0.30 (9H, s), 2.79 – 2.96 (1H, m), 3.06 – 3.22 (1H, m), 3.74 (4H, s), 4.06 – 4.24 (1H, m), 5.65 (1H, s), 6.55 (1H, s), 6.80 – 6.92 (2H, m), 7.11 – 7.26 (2H, m),

7.51 (1H, d, *J* = 9.4 Hz), 10.92 (1H, s), 11.97 (1H, s). LC/MS m/z 500.1 (M – H). Optical rotation: $[\alpha]^{25}_{D}$ –15.2 (c 0.128, MeOH). HPLC purity: 91.4%.

4-((1*R*)-1-((3,5-difluoro-4-(trimethylsilyl)phenyl)carbamoyl)-6-methoxy-3,4-dihydroisoquinolin-2(1*H*)-yl)-4-oxobutanoic acid (12). Compound **12** was prepared in a manner similar to that described for **15**, using dihydrofuran-2,5-dione in 95% yield as a colorless amorphous solid. ^{1}H NMR (300 MHz, DMSO-d_6) 0.29 (9H, s), 2.57 – 2.92 (6H, m), 3.03 – 3.23 (1H, m), 3.45 – 3.63 (1H, m), 3.73 (3H, s), 3.97 – 4.10 (1H, m), 5.56 – 5.70 (1H, m), 6.76 – 6.89 (2H, m), 7.13 – 7.28 (2H, m), 7.40 – 7.50 (1H, m), 10.63 – 10.87 (1H, m). LC/MS m/z 489.2 (M – H). Optical rotation: $[\alpha]^{25}_{D}$ +3.8 (c 0.252, MeOH). HPLC purity: 94.8%.

(2*Z*)-4-((1*R*)-1-((3,5-difluoro-4-(trimethylsilyl)phenyl)carbamoyl)-6-methoxy-3,4-dihydroisoquinolin-2(1*H*)-yl)-4-oxobut-2-enoic acid (13). Compound **13** was prepared in a manner similar to that described for **9**, using maleic acid in 12% yield as a colorless amorphous solid. ^{1}H NMR (300 MHz, DMSO-d_6) 0.30 (9H, s), 2.68 – 2.89 (1H, m), 2.92 – 3.08 (1H, m), 3.40 – 3.52 (1H, m), 3.73 (3H, s), 3.85 – 4.05 (1H, m), 5.70 (1H, s), 6.07 (1H, d, *J* = 12.1 Hz), 6.75 – 6.87 (3H, m), 7.20 – 7.31 (2H, m), 7.43 (1H, d, *J* = 8.3 Hz), 10.65 – 10.81 (1H, m), 12.82 (1H, brs). LC/MS m/z 487.2 (M – H). Optical rotation: $[\alpha]^{25}_{D}$ +73.0 (c 0.127, MeOH). HPLC purity: 96.9%.

(2*E*)-4-((1*R*)-1-((3,5-difluoro-4-(trimethylsilyl)phenyl)carbamoyl)-6-methoxy-3,4-dihydroisoquinolin-2(1*H*)-yl)-4-oxobut-2-enoic acid (14). Compound **14** was prepared in a manner similar to that described for **9**, using fumaric acid in 18% yield as a colorless amorphous solid. ^{1}H NMR (300 MHz, DMSO-d_6) 0.30 (9H, s), 2.78 – 2.93 (1H, m), 3.06 – 3.21 (1H, m), 3.60 – 3.71 (1H, m), 3.73 (3H, s), 4.08 – 4.21 (1H, m), 5.63 – 5.79 (1H, m), 6.51 – 6.62 (1H, m),

6.77 – 6.90 (2H, m), 7.13 – 7.25 (2H, m), 7.39 – 7.57 (2H, m), 10.84 (1H, s), 13.07 (1H, brs). LC/MS m/z 487.2 (M – H). Optical rotation: $[\alpha]^{25}_{D}$ +7.7 (c 0.127, MeOH). HPLC purity: 99.3%.

6-((1*R*)-1-((3,5-difluoro-4-(trimethylsilyl)phenyl)carbamoyl)-6-methoxy-3,4-dihydroisoquinolin-2(1*H*)-yl)-6-oxohexanoic acid (16). Compound **16** was prepared in a manner similar to that described for **15**, using oxepane-2,7-dione in 11% yield as a colorless amorphous solid. ^{1}H NMR (300 MHz, DMSO-d_6) 0.29 (9H, s), 1.41 – 1.67 (4H, m), 2.12 – 2.31 (1H, m), 2.36 – 2.61 (3H, m), 2.66 – 2.89 (1H, m), 3.00 – 3.19 (1H, m), 3.43 – 3.60 (1H, m), 3.72 (3H, s), 3.95 – 4.11 (1H, m), 5.61 (1H, s), 6.82 (2H, d, *J* = 9.8 Hz), 7.19 (2H, d, *J* = 9.8 Hz), 7.45 (1H, d, *J* = 8.3 Hz), 10.74 (1H, s), 11.97 (1H, s). LC/MS m/z 517.3 (M – H). Optical rotation: $[\alpha]^{25}_{D}$ –3.3 (c 0.253, MeOH). HPLC purity: 96.7%.

(1*R*)-2-(5-amino-5-oxopentanoyl)-*N*-(3,5-difluoro-4-(trimethylsilyl)phenyl)-6-methoxy-1,2,3,4-tetrahydroisoquinoline-1-carboxamide (17). To a stirred solution of **15** (200 mg, 0.40 mmol) and *N*,*N*'-diisopropylethylamine (0.20 ml, 1.19 mmol) in DMF (4.0 ml) was added ammonium chloride (25.4 mg, 0.48 mmol) and HATU (181 mg, 0.48 mmol) at room temperature. The mixture was stirred at room temperature for 3 h. The mixture was quenched with water and extracted with EtOAc. The organic layer was separated, washed with water and brine, dried over $MgSO_4$ and concentrated in vacuo. The residue was purified by column chromatography (silica gel, eluted with 0%–50% EtOAc in hexane) and recrystallized from EtOAc–hexane to give **17** (114 mg, 57 %) as colorless crystals. ^{1}H NMR (300MHz, DMSO-d_6) 0.29 (9H, s), 1.73 (2H, quin, *J* = 7.1 Hz), 2.05 – 2.16 (2H, m), 2.32 – 2.57 (2H, m), 2.70 – 2.88 (1H, m), 3.04 – 3.18 (1H, m), 3.43 – 3.58 (1H, m), 3.73 (3H, s), 3.94 – 4.08 (1H, m), 5.62 (1H, s), 6.71 (1H, brs), 6.77 – 6.87 (2H, m), 7.14 – 7.29 (3H, m), 7.46 (1H, d, *J* = 9.4 Hz), 10.76 (1H,

s). LC/MS m/z 502.3 (M – H). Optical rotation: $[\alpha]^{25}_{D}$ –7.6 (c 0.254, MeOH). HPLC purity: 99.3%.

5-((1*R*)-1-((3,5-difluoro-4-(trimethylsilyl)phenyl)carbamoyl)-6-methoxy-3,4-dihydroisoquinolin-2(1*H*)-yl)-3-methyl-5-oxopentanoic acid (18). Compound **18** was prepared in a manner similar to that described for **15**, using 4-methyldihydro-2*H*-pyran-2,6(3*H*)-dione in 46% yield as a colorless amorphous solid. ^{1}H NMR (300 MHz, DMSO-d_6) 0.82 – 0.99 (3H, m), 2.04 – 2.20 (1H, m), 2.21 – 2.41 (3H, m), 2.42 – 2.61 (1H, m), 2.75 – 2.89 (1H, m), 3.03 – 3.21 (1H, m), 3.45 – 3.59 (1H, m), 3.73 (3H, s), 3.97 – 4.10 (1H, m), 5.62 (1H, s), 6.78 – 6.85 (2H, m), 7.14 – 7.25 (2H, m), 7.46 (1H, d, *J* = 9.4 Hz), 10.77 (1H, s), 12.04 (1H, brs). LC/MS m/z 517.3 (M – H). Optical rotation: $[\alpha]^{25}_{D}$ +2.8 (c 0.127, MeOH). HPLC purity: 99.3%.

5-((1*R*)-1-((3,5-difluoro-4-(trimethylsilyl)phenyl)carbamoyl)-6-methoxy-3,4-dihydroisoquinolin-2(1*H*)-yl)-3,3-dimethyl-5-oxopentanoic acid (19). Compound **19** was prepared in a manner similar to that described for **15**, using 4,4-dimethyldihydro-2*H*-pyran-2,6(3*H*)-dione in 49% yield as a colorless amorphous solid. ^{1}H NMR (300 MHz, DMSO-d_6) 0.29 (9H, s), 1.09 (6H, d, *J* = 1.1 Hz), 2.25 – 2.44 (2H, m), 2.56 – 2.86 (2H, m), 3.04 – 3.19 (1H, m), 3.45 – 3.61 (1H, m), 3.73 (3H, s), 3.96 – 4.15 (2H, m), 5.57 – 5.70 (1H, m), 6.76 – 6.89 (2H, m), 7.14 – 7.25 (2H, m), 7.45 (1H, d, *J* = 9.1 Hz), 10.77 (1H, s), 11.93 (1H, brs). LC/MS m/z 531.3 (M – H). Optical rotation: $[\alpha]^{25}_{D}$ +7.3 (c 0.051, MeOH). HPLC purity: 97.5%.

5-((1*R*)-1-((3,5-difluoro-4-(trimethylsilyl)phenyl)carbamoyl)-6-methoxy-3,4-dihydroisoquinolin-2(1*H*)-yl)-3-hydroxy-3-methyl-5-oxopentanoic acid (20). Compound **20** was prepared in a manner similar to that described for **15**, using 4-hydroxy-4-methyldihydro-2*H*-

pyran-2,6(3*H*)-dione in 34% yield a pale-yellow amorphous solid. ^{1}H NMR (300 MHz, DMSO-d_6) 0.29 (9H, s), 1.24 – 1.30 (3H, m), 2.42 – 2.47 (1H, m), 2.71 – 2.87 (6H, m), 3.02 – 3.16 (1H, m), 3.52 – 3.64 (1H, m), 3.73 (3H, s), 3.96 – 4.16 (1H, m), 5.65 (1H, s), 6.76 – 6.88 (2H, m), 7.16 – 7.28 (2H, m), 7.39 – 7.50 (1H, m), 10.74 (1H, s). LC/MS m/z 535.5 (M + H). Optical rotation: $[\alpha]^{25}_D$ +8.6 (c 0.256, MeOH). HPLC purity: 98.5%.

(2-((1*R*)-1-((3,5-difluoro-4-(trimethylsilyl)phenyl)carbamoyl)-6-methoxy-3,4-dihydroisoquinolin-2(1*H*)-yl)-2-oxoethoxy)acetic acid (21). Compound **21** was prepared in a manner similar to that described for **15**, using 1,4-dioxane-2,6-dione in 29% yield a colorless amorphous solid. ^{1}H NMR (300MHz, DMSO-d_6) 0.30 (9H, s), 2.75 – 2.91 (1H, m), 2.99 – 3.17 (1H, m), 3.40 – 3.56 (1H, m), 3.73 (3H, s), 3.91 – 4.02 (1H, m), 4.11 (2H, s), 4.32 – 4.50 (2H, m), 5.61 (1H, s), 6.75 – 6.89 (2H, m), 7.20 (2H, d, J = 9.8 Hz), 7.40 – 7.50 (1H, m), 10.80 (1H, s), 12.66 (1H, brs). LC/MS m/z 505.2 (M – H). HPLC purity: 100%.

((2-((1*R*)-1-((3,5-difluoro-4-(trimethylsilyl)phenyl)carbamoyl)-6-methoxy-3,4-dihydroisoquinolin-2(1*H*)-yl)-2-oxoethyl)(methyl)amino)acetic acid (22). Compound **22** was prepared in a manner similar to that described for **15**, using 4-methylmorpholine-2,6-dione in 77% yield a colorless amorphous solid. ^{1}H NMR (300 MHz, DMSO-d_6) 0.30 (9H, s), 2.38 (3H, s), 2.72 – 2.89 (1H, m), 2.89 – 3.00 (1H, m), 3.01 – 3.20 (2H, m), 3.35 – 3.49 (1H, m), 3.51 – 3.66 (3H, m), 3.73 (3H, s), 4.06 – 4.22 (1H, m), 5.60 (1H, s), 6.72 – 6.86 (2H, m), 7.13 – 7.26 (2H, m), 7.39 – 7.50 (1H, m), 10.81 (1H, s). LC/MS m/z 520.4 (M + H). Optical rotation: $[\alpha]^{25}_D$ +15.5 (c 0.252, MeOH). HPLC purity: 95.2%.

(1*R*)-*N*-(3,5-difluoro-4-(trimethylsilyl)phenyl)-2-((2,4-dioxo-1,3-thiazolidin-5-yl)acetyl)-6-methoxy-1,2,3,4-tetrahydroisoquinoline-1-carboxamide (23). Compound **23** was prepared in

a manner similar to that described for **9**, using (2,4-dioxo-1,3-thiazolidin-5-yl)acetic acid in 52% yield as colorless crystals. ^{1}H NMR (300 MHz, DMSO-d_6) 0.29 (9H, s), 2.76 – 2.90 (1H, m), 3.08 – 3.22 (1H, m), 3.24 – 3.38 (2H, m), 3.39 – 3.58 (1H, m), 3.73 (3H, s), 3.94 – 4.09 (1H, m), 4.54 – 4.70 (1H, m), 5.61 (1H, s), 6.77 – 6.90 (2H, m), 7.12 – 7.27 (2H, m), 7.44 (1H, t, J = 8.3 Hz), 10.77 (1H, d, J = 11.7 Hz), 11.96 (1H, brs). LC/MS m/z 546.2 (M – H). Optical rotation: $[\alpha]^{25}_{D}$ +7.3 (c 0.253, MeOH). HPLC purity: 97.1%.

(*R*)-4-((2-((3,5-difluoro-4-(trimethylsilyl)phenyl)amino)-1-(4-methoxyphenyl)-2-oxoethyl)(methyl)amino)-4-oxobutanoic acid (11). Compound **11** was prepared in a manner similar to that described for **15**, using dihydrofuran-2,5-dione in 71% yield as a colorless amorphous solid. ^{1}H NMR (300 MHz, DMSO-d_6) 0.31 (9H, s), 2.43 – 2.49 (2H, m), 2.55 – 2.68 (2H, m), 2.77 (3H, s), 3.75 (3H, s), 6.19 (1H, s), 6.97 (2H, d, J = 8.7 Hz), 7.15 (2H, d, J = 8.7 Hz), 7.24 (2H, d, J = 9.8 Hz), 10.60 (1H, s), 12.07 (1H, brs). LC/MS m/z 477.1 (M – H). Optical rotation: $[\alpha]^{25}_{D}$ –154.1 (c 0.251, MeOH). HPLC purity: 100%.

***tert*-Butyl benzyl(2-hydroxyethyl)carbamate (37).** Boc_2O (16.7 g, 76.4 mmol) was added to a solution of 2-(benzylamino)ethanol (11.0 g, 72.8 mmol) in THF (220 ml) at room temperature. After being stirred at room temperature for 16 h, the reaction mixture was concentrated in vacuo. The residual oil was purified by column chromatography on silica gel (eluted with 10%–60% EtOAc in hexane) to give **37** (18.3 g, quant.) as a colorless oil. ^{1}H NMR (300 MHz, $CDCl_3$) 0.47 (9H, s), 3.03 (1H, brs), 3.40 (2H, brs), 3.65 – 3.75 (2H, m), 4.48 (2H, brs), 7.21 – 7.37 (5H, m). LC/MS m/z 152.2 (M + H – (Boc)).

***tert*-Butyl benzyl(2-(3-methoxyphenoxy)ethyl)carbamate (38).** 1.9 M DIAD (47.8 ml, 90.9 mmol) in toluene was added to a solution of **37** (18.3 g, 72.7 mmol), 3-methoxyphenol (7.52 g,

60.6 mmol) and triphenylphosphine (23.8 g, 90.9 mmol) in THF (250 ml) at 0 °C under Ar. After being stirred at room temperarure for 3 d, the reaction mixture was poured into water (500 ml) and extracted with EtOAc. The organic layer was washed with water and brine, dried over $MgSO_4$ and concentrated in vacuo. The residual oil was purified by column chromatography on silica gel (eluted with 2%–15% EtOAc in hexane) to give **38** (8.83 g, 41 %) as a colorless oil. ^{1}H NMR (300 MHz, $CDCl_3$) 1.41 – 1.53 (9H, m), 3.47 – 3.63 (2H, m), 3.78 (3H, s), 3.97 – 4.14 (2H, m), 4.57 (2H, brs), 6.39 – 6.53 (3H, m), 7.16 (1H, t, *J* = 8.1 Hz), 7.22 – 7.36 (5H, m). LC/MS m/z 258.2 (M + H – (Boc)).

***N*-Benzyl-2-(3-methoxyphenoxy)ethanamine (39).** Ice-cooled trifluoroacetic acid (30 ml) was added to **38** (8.83 g, 24.7 mmol) at room temperature. After being stirred at room temperature for 15 min, the reaction mixture was poured into iced water, basified (pH 8) by the careful addition of 8 N NaOH and K_2CO_3, and extracted with EtOAc. The organic layer was washed with water and brine, dried over $MgSO_4$ and concentrated in vacuo to give **39** (6.34 g, quant.) as a colorless oil. This product was subjected to the next reaction without further purification. NMR (300 MHz, $CDCl_3$) 1.71 (1H, brs), 3.02 (2H, t, *J* = 5.3 Hz), 3.78 (3H, s), 3.88 (2H, s), 4.08 (2H, t, *J* = 5.3 Hz), 6.46 – 6.53 (3H, m), 7.17 (1H, t, *J* = 8.1 Hz), 7.27 – 7.38 (5H, m). LC/MS m/z 258.2 (M + H).

Methyl (benzyl(2-(3-hydroxyphenoxy)ethyl)amino)(methoxy)acetate (40). A mixture of methyl 2-methoxyacetate (2.82 g, 27.1 mmol), *N*-bromosuccinimide (5.04 g, 28.3 mmol), AIBN (0.081 g, 0.49 mmol) and $PhCF_3$ (50 ml) was stirred at 80 °C for 5 h. After being cooled to room temperature, the insoluble substance was filtered off and washed with $^i Pr_2O$-hexane (1:2). The filtrate was concentrated in vacuo, and the residual oil was added to a solution of **39** (6.34 g, 24.6 mmol) and *N*,*N*-diisopropylethylamine (5.15 ml, 29.6 mmol) in THF (60 ml) at room

temperature. After being stirred at room temperature for 1 h, the reaction mixture was poured into aqueous $NaHCO_3$ and extracted with EtOAc. The organic layer was washed with water and brine, dried over $MgSO_4$ and concentrated in vacuo. The residual oil was purified by column chromatography on NH silica gel (eluted with 2%–20% EtOAc in hexane) to give **40** (6.72 g, 76 %) as a colorless oil. This product was subjected to the next reaction without further purification. ^{1}H NMR (300 MHz, $CDCl_3$) 3.12 (2H, td, *J* = 5.9, 1.5 Hz), 3.39 (3H, s), 3.77 (3H, s), 3.77 (3H, s), 3.87 – 4.08 (4H, m), 4.48 (1H, s), 6.38 – 6.53 (3H, m), 7.15 (1H, t, *J* = 8.1 Hz), 7.24 – 7.39 (5H, m). LC/MS m/z 360.3 (M + H).

Methyl 4-benzyl-8-methoxy-2,3,4,5-tetrahydro-1,4-benzoxazepine-5-carboxylate (41). To a solution of **40** (6.72 g, 18.7 mmol) in CH_3CN (75 mL) was added chlorotrimethylsilane (2.85 ml, 22.4 mmol) at 0 °C, and the reaction mixture was stirred at room temperature for 1 h. The reaction mixture was poured into aqueous $NaHCO_3$ and extracted with EtOAc. The organic layer was washed with water and brine, dried over $MgSO_4$ and concentrated in vacuo. The residue was purified by column chromatography on silica gel (eluted with 3%–80% EtOAc in hexane) to give **41** (3.65 g, 60 %) as a colorless oil. ^{1}H NMR (300 MHz, $CDCl_3$) 2.97 (1H, ddd), 3.56 (1H, ddd, *J* = 14.5, 8.7, 2.5 Hz), 3.67 – 3.82 (7H, m), 3.95 (1H, d, *J* = 13.6 Hz), 3.98 – 4.06 (1H, m), 4.12 – 4.20 (1H, m), 4.49 (1H, s), 6.58 (1H, dd), 6.61 (1H, d), 6.87 (1H, d, *J* = 8.3 Hz), 7.23 – 7.38 (5H, m). LC/MS m/z 328.2 (M + H).

4-*tert*-Butyl 5-methyl 8-methoxy-2,3-dihydro-1,4-benzoxazepine-4,5(5*H*)-dicarboxylate (42). A solution of **41** (5.67 g, 17.3 mmol) in MeOH (115 ml) was hydrogenated in the presence of 20% $Pd(OH)_2$-C (50% wet) (1.9 g, 6.23 mmol) at room temperature under ordinary pressure for 2.5 h. After removal of the catalyst by filtration, the filtrate was concentrated in vacuo. The evaporation was repeated after the addition of toluene. The residual oil was dissolved in THF (45 ml), and Boc_2O (3.86 g, 17.7 mmol) was added thereto at room temperature. After being stirred

at room temperature for 2 h, the reaction mixture was concentrated in vacuo to give crystals, which were collected by filtration and washed with $^{i}Pr_2O$-hexane to give **42** (4.48 g, 77 %) as colorless powder. ^{1}H NMR (300 MHz, $CDCl_3$) 1.44 – 1.49 (9H, m), 3.69 – 3.73 (3H, m), 3.74 – 4.00 (6H, m), 4.23 – 4.38 (1H, m), 5.54 – 5.97 (1H, m), 6.53 – 6.59 (1H, m), 6.59 – 6.66 (1H, m), 7.09 – 7.24 (1H, m). LC/MS m/z 238.2 (M + H – (Boc)).

4-(*tert*-Butoxycarbonyl)-8-methoxy-2,3,4,5-tetrahydro-1,4-benzoxazepine-5-carboxylic acid (43). 2 *N* lithium hydroxide (39.8 ml, 79.7 mmol) was added to a mixture of **42** (4.48 g, 13.3 mmol), MeOH (21 ml) and THF (21 ml) at room temperature. After being stirred at room temperature for 1.5 h (to give a solution), the reaction mixture was poured into iced water (200 ml), acidified (pH 3) with 2 *N* HCl and extracted with EtOAc–THF (4:1). The organic layer was washed with water and brine, dried over $MgSO_4$ and concentrated in vacuo to give crystals, which were collected by filtration and washed with $^{i}Pr_2O$-hexane to give **43** (4.04 g, 94 %) as colorless powder. ^{1}H NMR (300 MHz, $CDCl_3$) 1.46 (9H, s), 3.71 – 3.81 (4H, m), 3.86 – 3.97 (2H, m), 4.23 – 4.39 (1H, m), 5.54 – 6.00 (1H, m), 6.54 – 6.67 (2H, m), 7.14 – 7.24 (1H, m). LC/MS m/z 322.2 (M – H)

***tert*-Butyl 5-((3,5-difluoro-4-(trimethylsilyl)phenyl)carbamoyl)-8-methoxy-2,3-dihydro-1,4-benzoxazepine-4(5*H*)-carboxylate (44).** T3P, 1.7 M solution in EtOAc (1.91 ml, 3.21 mmol) was added to a solution of **43** (692 mg, 2.14 mmol), 3,5-difluoro-4-(trimethylsilyl)aniline (431 mg, 2.14 mmol), *N*,*N*-diisopropylethylamine (1.86 ml, 10.7 mmol) and DMAP (288 mg, 2.35 mmol) in EtOAc (17 ml) at room temperature. After being stirred at 65 °C for 15 h, the reaction mixture was poured into water and extracted with EtOAc. The organic layer was washed with water and brine, dried over $MgSO_4$ and concentrated in vacuo. The residual oil was purified by column chromatography on silica gel (eluted with 5%– 30% EtOAc in hexane) to give **44** (924

mg, 85 %) as a colorless amorphous solid. ^{1}H NMR (400 MHz, $CDCl_3$) 0.31 (9H, s), 1.47 (9H, s), 3.66 – 3.78 (1H, m), 3.81 (3H, s), 3.86 – 3.95 (2H, m), 4.33 (1H, brs), 5.38 – 5.98 (1H, m), 6.65 (1H, d, *J* = 2.3 Hz), 6.70 (1H, dd, *J* = 8.3, 2.3 Hz), 6.95 (2H, d, *J* = 8.7 Hz), 7.19 – 7.25 (1H, m), 7.46 – 7.97 (1H, m). LC/MS m/z 505.2 (M – H).

***N*-(3,5-Difluoro-4-(trimethylsilyl)phenyl)-8-methoxy-2,3,4,5-tetrahydro-1,4-benzoxazepine-5-carboxamide (45).** Ice-cooled trifluoroacetic acid (10 ml) was added to **44** (919 mg, 1.81 mmol). After being stirred at room temperature for 2 min, the reaction mixture was poured intoiced saturated aqueous $NaHCO_3$, basified (pH 8) by the careful addition of K_2CO_3 and extracted with EtOAc. The organic layer was washed with water and brine, dried over $MgSO_4$ and concentrated in vacuo to give crystals, which were collected by filtration and washed with hexane to give **45** (652 mg, 88 %) as colorless powder. ^{1}H NMR (300 MHz, $CDCl_3$) 1.74 (1H, brs), 3.13 – 3.29 (2H, m), 3.80 (3H, s), 3.96 – 4.13 (2H, m), 4.69 (1H, s), 6.62 – 6.67 (2H, m), 7.08 – 7.16 (2H, m), 7.17 – 7.21 (1H, m), 9.16 (1H, s). LC/MS m/z 407.2 (M + H).

(5*R*)-*N*-(3,5-difluoro-4-(trimethylsilyl)phenyl)-4-((3-hydroxy-1,2-oxazol-5-yl)carbonyl)-8-methoxy-2,3,4,5-tetrahydro-1,4-benzoxazepine-5-carboxamide (10). HATU (245 mg, 0.64 mmol) was added to a solution of **45** (218 mg, 0.54 mmol), 3-hydroxyisoxazole-5-carboxylic acid (72.7 mg, 0.56 mmol) and *N*,*N*-diisopropylethylamine (0.187 ml, 1.07 mmol) in DMF (2.6 ml) at room temperature. After being stirred at room temperature for 15 h, the reaction mixture was poured into water and extracted with EtOAc. The organic layer was washed with water and brine, dried over $MgSO_4$ and concentrated in vacuo. The residual oil was purified by column chromatography on silica gel (eluted with 30%–100% EtOAc in hexane) to give crystals, which were collected by filtration and washed with $^iPr_2O$-hexane to give *N*-(3,5-difluoro-4-(trimethylsilyl)phenyl)-4-(3-hydroxyisoxazole-5-carbonyl)-8-methoxy-2,3,4,5-

tetrahydrobenzo[*f*][1,4]oxazepine-5-carboxamide (114.5 mg, 41 %) as colorless powder. The product (100 mg) was subjected to preparative SFC (Column: CHIRALPAK AS-H, Eluent: CO_2/ethanol =840/160 (v/v), Flow rate: 75 mL/min, Pressure: 0.1 Mpa, Detector&sens.: UV220 nM, Temperature: 35 °C). The factions with a shorter retention time gave the title compound **10** (30.3 mg, 30%) with > 99%ee as colorless amorphous solid. ^{1}H NMR (300 MHz, DMSO-d_6) 0.31 (9H, s), 3.74 (3H, s), 3.78 – 4.13 (3H, m), 4.29 – 4.44 (1H, m), 5.86 – 6.05 (1H, m), 6.51 (1H, s), 6.54 – 6.63 (1H, m), 6.64 – 6.76 (1H, m), 7.20 – 7.38 (3H, m), 10.36 (1H, s), 11.99 (1H, s). LC/MS m/z 518.2 (M + H). Optical rotation: $[\alpha]^{25}_{D}$ –44.8 (c 0.252, MeOH). HPLC purity: 99.6%.

X-ray structure analysis of tartrate of compound 31

Crystal data for tartrate of compound **31**: $C_{20}H_{25}F_2N_2O_2Si^+ \cdot C_{20}H_{17}O_8^-$, *MW* = 776.86; crystal size, 0.25 x 0.19 x 0.05 mm; colourless, plate; orthorhombic, space group $P2_12_12_1$, a = 8.63289(12) Å, b = 13.3829(2) Å, c = 33.4183(6) Å, $\alpha = \beta = \gamma = 90°$, V = 3860.92(10) Å^3, Z = 4, Dx = 1.336 g/cm^3, T = 100 K, μ = 1.139 mm^{-1}, λ = 1.54187 Å, R_1 = 0.045, wR_2 = 0.115, Flack Parameter[30] = 0.02(2).

All measurements were made on a Rigaku XtaLAB P200 diffractometer using multi-layer mirror monochromated Cu-Kα radiation. The structure was solved by direct methods with SIR2008[31] and was refined using full-matrix least-squares on F^2 with SHELXL-2014/7.[32] All non-H atoms were refined with anisotropic displacement parameters.

CCDC 1575732 for tartrate of compound **31** contains the supplementary crystallographic data for this paper. These data can be obtained free of charge from The Cambridge Crystallographic

Data Centre via http://www.ccdc.cam.ac.uk/Community/Requestastructure/Pages/DataRequest.aspx?.

Biology.

Binding assay

The binding activity of the test compound to ROR t was measured by a time resolved fluorescence resonance energy transfer method (TR-FRET) utilizing histidine-tagged ROR t, a fluorescent-labeled our original synthetic ligand[33] and a terbium-labeled anti-histidine tag antibody (Invitrogen). First, a test compound diluted with an assay buffer (20 mM Tris-HCl (pH 7.5), 100 mM NaCl, 1 mM DTT, 0.1% BSA) was added to a 384 well plate by 3 μL. Then, ROR t diluted with an assay buffer to 240 nM was added by 3 μL, after which the fluorescent-labeled synthetic ligand diluted with the assay buffer to 12 μM was added by 3 μL, and the mixture was stood at room temperature for 20 min. Thereafter, a terbium-labeled anti-histidine tag antibody diluted with the assay buffer to 8 nM was added by 3 μL. The mixture was stood at room temperature for 20 min, and fluorescence intensity (excitation wavelength 320 nm, fluorescence wavelength 520 nm, delay time 100 microseconds) was measured by Envision (PerkinElmer). The results (binding inhibitory rate of the fluorescent-labeled synthetic ligand to ROR t at test compound 1 μM) measured by the above-mentioned method are shown in Table 1–2.

Reporter gene assay

The Jurkat cells used for the reporter test were cultured in a culture medium (RPMI (Invitrogen), 10% FCS (AusGeneX), 100 U/mL penicillin, 100 μg/mL streptomycin). On the day of the test, 4×107 cells were recovered by a centrifugal operation (1000 rpm, 5 min.) and

suspended in PBS (phosphate buffered saline) (Invitrogen). Thereafter, the cells were recovered again by a centrifugal operation, and suspended in 2 mL of R buffer (NEON transfection kit, Invitrogen). Then, a reporter vector (53 μg) wherein a human IL-17 ROR response element was inserted into the upstream of luciferase of pGL 4.28 (Promega), and a vector (27 μg) wherein ROR t sequence was inserted into the downstream of CMV promoter were added to the cell suspension. Gene transfer was performed by Electroporation apparatus (NEON, Invitrogen) under the conditions of pulse voltage 1350 V, interval 10 milliseconds, number of times 3. The cells after gene transfer were suspended in 40 mL of a reaction medium (RPMI, 10% Lipid reduced FCS (HyClone), 10 mM HEPES (pH 7.5), 100 U/mL penicillin, 100 μg/mL streptomycin, 5 μM lovastatin), and plated in a 96 well plate by 90 μL. A test compound diluted with the reaction medium was added by 10 μL, and the cells were cultured overnight in an incubator. Bright-Glo (Promega) was added by 100 μL, and the mixture was stirred at room temperature for 10 min, and the luminescence level was measured by Envision (PerkinElmer).

The results (luminescence level inhibitory rate at test compound 3 μM) measured by the above-mentioned method are shown in Table 1–2.

PD assay, IL-23-induced cytokine production in mice

Recombinant mouse IL-23 (500 ng/10 μL, prepared by Takeda Pharmaceutical Company Limited.) in PBS or PBS (10 μL, negative control group) was intradermally injected in the ears of Balb/c mice (male, 7 weeks-old) under anesthesia with isoflurane. Compound **15** suspended in 0.5% methylcellulose (MC) or 0.5% MC was orally administered to the mice 30 min before and 8 hours after the IL-23 injection. Twenty-four hours after the IL-23 injection, mice were euthanized, and their ear samples were collected by 5-mm biopsy punches, and the ear samples were immersed in RNAlater (QIAGEN, Germany) for at least 18 hours. RNA extraction from the

ear tissue and quantitative PCR were performed as follows. The RNAlater-treated ear tissue was homogenized in 350 μL of RLT buffer (RNeasy mini kit, QIAGEN, Germany) and treated (55 °C, 10 min) with Proteinase K (QIAGEN, Germany). Total RNA was then extracted according to the RNeasy mini kit protocol. The RNA thus obtained was then reverse transcribed into cDNA using the High-Capacity RNA-to-cDNA kit (Applied Biosystems, USA), and the amount of each cytokine expression was measured by real-time PCR (Viia7TM, Applied Bio systems, USA). The PCR buffer used was TaqMan Fast Advanced Master Mix (Applied Bio systems, USA), and TaqMan Gene Expression Assays (Applied Biosystems, Mm00439618_m1 (IL-17A) and 4352341E (-actin)) were used for each gene detection. Expression level of each gene was normalized to the expression level of -actin gene, and the percent inhibition of IL-17A gene expression with the test compound was then calculated.

The results (percent inhibition of IL-17A gene expression with oral administration of compound **15**) measured by the above-mentioned method are shown in Figure 5.

Cassette dosing in mice

All experiments were conducted in accordance with the regulations of Animal Care and Use Committee of the Takeda Pharmaceutical Company Ltd. Test compounds were administered as a cassette dosing to mice. After oral administration, blood samples were collected. The blood samples were centrifuged to obtain the plasma fraction. The plasma samples were deproteinized with acetonitrile containing an internal standard. After centrifugation, the supernatant was diluted with LC mobile phase and centrifuged again. The compound concentrations in the supernatant were measured by LC/MS/MS.

Acknowledgment. We thank Keiji Kamiyama, Takashi Ichikawa, Masato Yoshida, Ayumu Sato, and Yusuke Sasaki for discussion on medicinal chemistry. We thank Yumi N Imai and Kazuko Yonemori for discussion on computational chemistry. We thank Mitsuyoshi Nishitani and Miyuki Yokomizo for structural analysis of synthesized compound.

References

(1) (a) Beringer, A.; Noack, M.; Miossec, P. IL-17 in chronic inflammation: from discovery to targeting. *Trends in molecular medicine*. **2016**, *22*, 230–241. (b) Miossec, P.; Kolls, J. K. Targeting IL-17 and TH17 cells in chronic inflammation, *Nature reviews Drug discovery*, **2012**, *11*, 763–776. (c) Wilke, C. M.; Bishop, K.; Fox, D.; Zou, W. Deciphering the role of Th17 cells in human disease, *Trends in immunology*, **2011**, *32*, 603–611.

(2) (a) Rovedatti, L.; Kudo, T.; Biancheri, P.; Sarra, M.; Knowles, C. H.; Rampton, D. S.; Corazza, G. R.; Monteleone, G.; Di Sabatino, A.; Macdonald, T. T. Differential regulation of interleukin 17 and interferon production in inflammatory bowel disease. *Gut*. **2009**, *58*, 1629–1636. (b) Duerr, R. H.; Taylor, K. D.; Brant, S. R.; Rioux, J. D.; Silverberg, M. S.; Daly, M. J.; Steinhart, A. H.; Abraham, C.; Regueiro, M.; Griffiths, A. A genome-wide association study identifies IL23R as an inflammatory bowel disease gene. *Science*, **2006**, *314*, 1461–1463.

(3) Kotake, S.; Udagawa, N.; Takahashi, N.; Matsuzaki, K.; Itoh, K.; Ishiyama, S.; Saito, S.; Inoue, K.; Kamatani, N.; Gillespie, M. T. IL-17 in synovial fluids from patients with rheumatoid arthritis is a potent stimulator of osteoclastogenesis. *The Journal of clinical investigation*. **1999**, *103*, 1345–1352.

(4) Kebir, H.; Ifergan, I.; Alvarez, J. I.; Bernard, M.; Poirier, J.; Arbour, N.; Duquette, P.; Prat, A. Preferential recruitment of interferon- -expressing TH17 cells in multiple sclerosis. *Ann. Neurol.* **2009**, *66*, 390–402.

(5) (a) Campa, M.; Mansouri, B.; Warren, R.; Menter, A. A review of biologic therapies targeting IL-23 and IL-17 for use in moderate-to-severe plaque psoriasis. *Dermatol.Ther.* **2016**, *6*, 1–12. (b) Nair, R. P.; Duffin, K. C.; Helms, C.; Ding, J.; Stuart, P. E.; Goldgar, D.; Gudjonsson, J. E.; Li, Y.; Tejasvi, T.; Feng, B. J. Genome-wide scan reveals association of psoriasis with IL-23 and NF- B pathways, *Nature genetics*. **2009**, *41*, 199–204.

(6) Farahnik, B.; Beroukhim, K.; Zhu, T. H.; Abrouk, M.; Nakamura, M.; Singh, R.; Lee, K.; Bhutani, T.; Koo, J. Ixekizumab forthe treatment of psoriasis: a review of phaseⅢtraials. *Dermatol Ther*. **2016**, *6*, 25–37.

(7) Sanford, M.; McKeage, K.; Secukinumab: first global approval. *Drugs.* **2015**, *75*, 329–338.

(8) Letko, E.; Yeh, S.; Foster, C. S.; Pleyer, U.; Brigell, M.; Grosskreutz, C. L. AIN457A2208 Study Group. Efficacy and safety of intravenous secukinumab in noninfectious uveitis requiring steroid-sparing immunosuppressive therapy. *Ophthalmology.* **2015**, *122*, 939–948.

(9) Ivanov, I. I.; Mackenzir, B. S.; Zhou, L.; Tadokoro, C. E.; Lepelley, A.; Lafallie, J. J.; Cua, D. J.; Littman, D. R. The orphan nuclear receptor ROR t directs the differentiation program of proinflammatory IL-17+ T helper cells. *Cell.* **2006**, *126*, 1121–1133.

(10) Annunziato, F.; Cosmi, L.; Santarlasci, V.; Maggi, L.; Liotta, F.; Mazzinghi, B.; Parente, E.; Filì, L.; Ferri, S.; Frosali, F.; Giudici, F.; Romagnani, P.; Parronchi, P.; Tonelli, F.; Maggi,

E.; Romagnani, S. Phenotypic and functional features of human Th17 cells. *J. Exp. Med.* **2007**, *204*, 1849–1861.

(11) He, Y. W.; Deftos, M. L.; Ojala, E.; W.; Bevan, M. J. ROR t, a novel isoform of an orphan receptor, negatively regulates Fas ligand expression and IL-2 production in T cells. *Immunity.* **1998**, *9*, 797–806.

(12) Yang, J.; Sundrud, M. S.; Skepner, J.; Yamagata, T. Targeting Th17 cells in autoimmune diseases, *Trends in pharmacological sciences*. **2014**, *35*, 493–500.

(13) Sutton, C. E.; Mielke, L. A.; Mills, K. H. IL-17-producing T cells and innate lymphoid cells. *Eur. J. Immunol.* **2012**, *42*, 2221–2231.

(14) Huh, J. R.; Leung, M. W. L.; Huang, P.; Ryan, D. A.; Krout, M. R.; Malapaka, R. R. V.; Chow, J.; Manel, N.; Ciofani, M.; Kim, S. V.; Cuesta, A.; Santori, F. R.; Lafaille, J. J.; Xu, H. E.; Gin, D. Y.; Rastinejad, F.; Littman, D. R. Digoxin and its derivatives suppress TH17 cell differentiation by antagonizing ROR t activity. *Nature* **2011**, *472*, 486–490.

(15) Xu, T.; Wang, X.; Zhong, B.; Nurieva, R. I.; Ding, S.; Dong, C. Ursolic acid suppress interleukin-17 (IL-17) production by selectively antagonizing the function of ROR t protein. *J. Biol. Chem* **2011**, *286*, 22707–22710.

(16) Wang, Y.; Cai, W.; Cheng, Y.; Yang, T.; Liu, Q.; Zhang, G.; Meng, Q.; Han, F.; Huang, Y.; Zhou, L.; Xiang, Z.; Zhao, Y. G.; Xu, Y.; Cheng, Z.; Lu, S.; Wu, Q.; Xiang, J. N.; Elliott, J. D.; Leung, S.; Ren, F.; Lin, X. Discovery of Biaryl Amides as Potent, Orally Bioavailable, and CNS Penetrant ROR t inhibitors. *ACS Med. Chem. Lett.* **2015**, *6*, 787–792.

(17) Fauber, B. P.; Gobbi, A.; Robarge, K.; Zhou, A.; Barnard, A.; Cao, J.; Deng, Y.; Eidenschenk, C.; Everett, C.; Ganguli, A.; Hawkins, J.; Johnson, A. R.; La, H.; Norman, M.; Salmon, G.; Summerhill, S.; Ouyang, W.; Tang, W.; Wong, H. Discovery of imidazo[1,5-*a*]pyridines and –pyrimidines as potent and selective RORc inverse agonists. *Bioorg. Med. Chem. Lett*. **2015**, *25*, 2907–2912.

(18) Hirata, K.; Kotoku, M.; Seki, N.; Maeba, T.; Maeda, K.; Hirashima, S.; Sakai, T.; Obika, S.; Hori, A.; Hase, Y.; Yamaguchi, T.; Katsuda, Y.; Hata, T.; Miyagawa, N.; Arita, K.; Nomura, Y.; Asahina, K.; Aratsu, Y.; Kamada, M.; Adachi, T.; Noguchi, M.; Doi, S.; Crowe, P.; Bradley, E.; Steensma, R.; Tao, H.; Fenn, M.; Babine, R.; Li, X.; Thacher, S.; Hashimoto, H.; Shiozaki, M. SAR Exploration Guided by LE and Fsp^3: Discovery of a Selective and Orally Efficacious ROR Inhibitor. *ACS Med. Chem. Lett.* **2016**, *7*, 23–27.

(19) (a) Chao, J.; Enyedy, I.; Van Vloten, K.; Marcotte, D.; Guertin, K.; Hutchings, R.; Powell, N.; Jones, H.; Bohnert, T.; Peng, C. C.; Silvian, L.; Hong, V. S.; Little, K.; Banerjee, D.; Peng, L.; Taveras, A.; Viney, J. L.; Fontenot, J. Discovery of biaryl carboxylamides as potent ROR inverse agonists. *Bioorg. Med. Chem. Lett.* **2015**, *25*, 2991–2997. (b) Solt, L. A.; Kumar, N.; Nuhant, P.; Wang, Y.; Lauer, J. L.; Liu, J.; Istrate, M. A.; Kamenecka, T. M.; Roush, W. R.; Vidovic, D.; Schurer, S. C, Xu, J.; Wagoner, G.; Drew, P. D.; Griffin, P. R. Burris, T. P. Suppression of TH17 differentiation and autoimmunity by a synthetic ROR ligands. *Nature* **2011**, *472*, 491-494.

(20) (a) Vitae Pharmaceuticals press release.
http://ir.vitaepharma.com/phoenix.zhtml?c=219654&p=irol-newsArticle&ID=2149044
Accessed 29 March 2016.

(b) An ascending multiple dose study with VTP-43742 in healthy volunteers and psoriatic patients.

https://clinicaltrials.gov/ct2/show/NCT02555709?term=VTP-43742&rank=1

Accessed 29 March 2016.

(c) Gege C. Retinoid-related orphan receptor gamma t (RORγt) inhibitors from Vitae Pharmaceuticals (WO2015116904) and structure proposal for their Phase I candidate VTP-43742. *Expert Opin. Ther. Pat.* **2016**, *26*, 737–744.

(21) Phenex Pharmaceuticals AG press release.

http://www.phenex-pharma.com/pdf/Phenex_Janssen_Ph1_eng_2017_final.pdf

Accessed 10 July 2017.

(22) (a) Arrien Pharmaceuticals news and scientific events. http://www.arrienpharma.com/news.php

Accessed 26 May 2016. (b) Vankayalapati, H.; Yerramreddy, V. WO 2015/038350, 2015.

(23) Orphagen Pharmaceuticals and Japan Tabaco Inc press release.

http://www.orphagen.com/japan-tobacco-initiates-phase-clinical-trial-novel-small-molecule-therapeutic-autoimmune-allergic-diseases/

Accessed 31 August 2016.

(24) Junya Shirai, Yoshihide Tomata, Mitsunori Kono, Atsuko Ochida, Yoshiyuki Fukase, Ayumu Sato, Shinichi Masada, Tetsuji Kawamoto, Kazuko Yonemori, Ryoukichi Koyama, Hideyuki Nakagawa, Masaharu Nakayama, Keiko Uga, Akira Shibata, Keiko Koga, Toshitake Okui, Mikio Shirasaki, Robert Skene, Bi Ching Sang, Isaac Hoffman, Wes Lane, Yasushi Fujitani, Masashi Yamasaki, and Satoshi Yamamoto. Discovery of orally efficacious ROR t inverse agonists. Part 1.: Identification of novel phenylglycinamides as lead scaffolds, *submitted*

(25) Veber, D. F.; Johnson, S. R.; Cheng, H. Y.; Smith, B. R.; Ward, K. W.; Kopple, K. D. Molecular properties that influence the oral bioavailability of drug candidates, *Journal of medicinal chemistry*, **2002**, *45*, 2615–2623.

(26) Lima, L. M.; Barreiro, E. J. Bioisosterism: A Useful Strategy for Molecular Modification and Drug Design. *Current Medicinal Chemistry* **2005**, *12*, 23–49.

(27) Keiko Uga et al. *in preparation*

(28) Bunin, B. A.; Dener, J. M.; Kelly, D. E.; Paras, N. A.; Tario, J. D.; Tushup, S. P. Solid-Phase Synthesis of 1-Substituted Tetrahydroisoquinoline Derivatives Employing BOC-Protected Tetrahydroisoquinoline Carboxylic Acids. *J. Comb. Chem.* **2004**, *6*, 487–496.

(29) Sakai, N.; Watanabe, A.; Ikeda, R.; Nakaike, Y.; Konakahara, T. Me_3SiCl-promoted intramolecular cyclization of aromatic compounds tethered with *N,O*-acetals leading to the facile preparation of 1,4-benzodiazepine skeletons. Tetrahedron **2010**, *66*, 8837–8845.

(30) Flack, H. D. *Acta Cryst. A* **1983**, *39*, 876.

(31) Burla, M. C., Caliandro, R., Camalli, M., Carrozzini, B., Cascarano, G. L., De Caro, L., Giacovazzo, C., Polidori, G. Siliqi, D. and Spagna R. *J. Appl. Cryst* **2007**, *40*, 609.

(32) Sheldrick, G.M. *Acta Cryst. A*, **2008**, *64*, 112.

(33) Yamamoto, S. et al., WO2015002231

Graphical Abstract

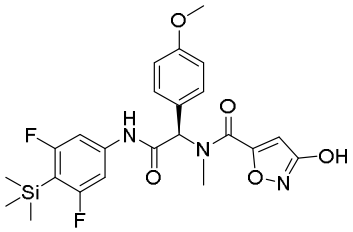

7

Binding IC_{50} = 4.3 nM
Reporter gene IC_{50} = 13 nM
Mouse PK (p.o. at 1mg/kg)
$AUC_{0\text{-}24h}$ = 374 ng·h/mL
F = 18%

1. SBDD-guided scaffold hopping
2. Replacement with a carboxylic acid tether

Remarkable improvement of
PK profile and in vivo efficacy

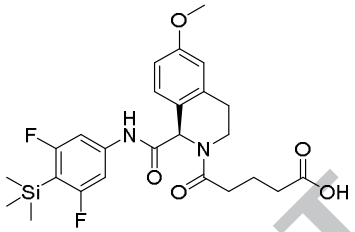

15

Binding IC_{50} = 3.0 nM
Reporter gene IC_{50} = 23 nM
Mouse PK (p.o. at 1mg/kg)
$AUC_{0\text{-}24h}$ = 6894 ng·h/mL
F = 94%

Table 1. In vitro activities and their PK profiles of derivatives modifying core scaffold and acyl tether

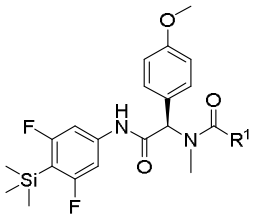

X

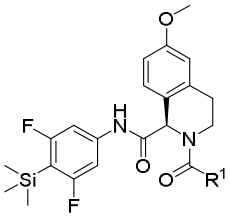

Y

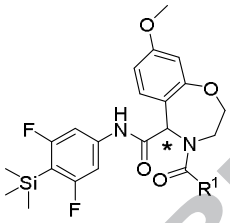

Z

Compound	Scaffold	R^1	Binding[a]	Reporter gene[b]	mouse PK[d]	
			IC_{50} (nM) [95%CI][c]	IC_{50} (nM) [95%CI][c]	$AUC_{0\text{-}8h}$ (μg·h/mL)	*F* (%)
8a	**X**	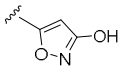	4.3 [3.4–5.5]	13 [10–16]	374	18
9	**Y**	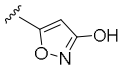	5.3 [4.7–5.9]	6.1 [3.6–11]	200	11
10[e]	**Z**	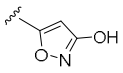	2.8 [2.5–3.1]	40 [20–83]	29.5	9.0
11	**X**	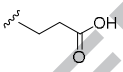	7.5 [5.9–9.5]	220 [150–310]	162	8.5
12	**Y**	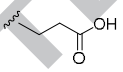	4.2 [3.6–4.8]	54 [42–70]	2500	51

[a] Displacement assay of BODIPY-labeled ligand with apo RORγt

[b] Inhibition of RORγt transcriptional activity in human Jurkat cells

[c] 95% confidence intervals (CI) in duplicate (n = 2)

[d] The values shown as means of three determinations (1 mg/kg, po)

[e] Compound **10** is eutomer

Table 2. In vitro activities and their PK profiles of derivatives modifying the acyl tether

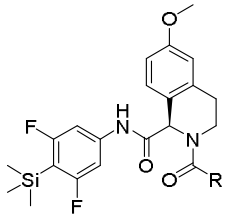

Compound	R^1	Binding[a]	Reporter gene[b]	mouse PK[d]	
		IC_{50} (nM) [95%CI][c]	IC_{50} (nM) [95%CI][c]	$AUC_{0\text{-}8h}$ (μg·h/mL)	*F* (%)
12	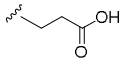	4.2 [3.6–4.8]	54 [41–70]	2500	51
13	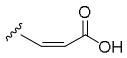	17 [10–27]	320 [260–410]	N.T.	N.T.
14	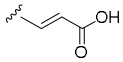	4.1 [3.4–4.9]	38 [29–49]	619	51
15	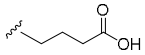	3.0 [2.4–3.8]	23 [19–29]	6894	94
16	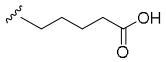	6.6 [5.6–7.8]	24 [19–31]	1031	84
17	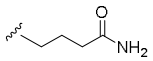	3.1 [2.3–4.0]	6.7 [4.7–9.6]	92	14
18	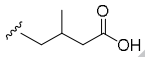	3.8 [3.1–4.7]	19 [12–30]	2498	65
19	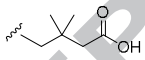	5.6 [4.9–6.5]	46 [28–78]	2273	40
20	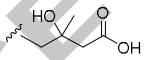	4.5 [3.8–5.3]	32 [25–41]	159	34
21	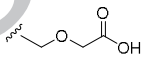	3.5 [3.0–4.0]	140 [97–190]	N.T.	N.T.
22	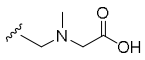	7.8 [6.5–9.4]	220 [150–320]	N.T.	N.T.
23	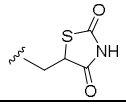	7.6 [6.4–9.2]	41 [28–62]	120	13

[a] Displacement assay of BODIPY-labeled ligand with apo RORγt

[b] Inhibition of RORγt transcriptional activity in human Jurkat cells

[c] 95% confidence intervals (CI) in duplicate (n = 2)

[d] The values shown as means of three determinations (1 mg/kg, po)

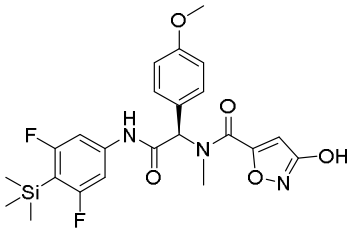

7

Binding IC_{50} = 4.3 nM
Reporter gene IC_{50} = 13 nM
Mouse PK (p.o. at 1mg/kg)
$AUC_{0\text{-}24h}$ = 374 ng·h/mL
F = 18%

1. SBDD-guided scaffold hopping
2. Replacement with a carboxylic acid tether

Remarkable improvement of
PK profile and in vivo efficacy

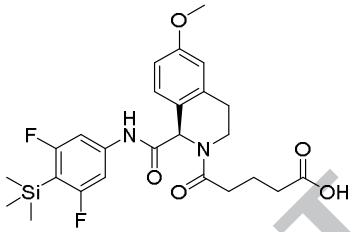

15

Binding IC_{50} = 3.0 nM
Reporter gene IC_{50} = 23 nM
Mouse PK (p.o. at 1mg/kg)
$AUC_{0\text{-}24h}$ = 6894 ng·h/mL
F = 94%